STRUCTURES AND CHEMISTRY OF AMINO AND NITRO FURAZANS

by

Royce Weldon Beal

A thesis submitted to the Faculty of the University of Delaware in partial fulfillment of the requirements for the degree of Master of Science in Chemistry and Biochemistry

Summer 2000

REPORT DOCUMENTATION PAGE

Form Approved
OMB No. 0704-0188

1. AGENCY USE ONLY *(Leave blank)*	2. REPORT DATE	3. REPORT TYPE AND DATES COVERED
	1.Jun.00	THESIS

4. TITLE AND SUBTITLE
STRUCTURES AND CHEMISTRY OF AMINO AND NITRO FURAZANS

5. FUNDING NUMBERS

6. AUTHOR(S)
CAPT BEAL ROYCE W

7. PERFORMING ORGANIZATION NAME(S) AND ADDRESS(ES)
UNIVERSITY OF DELAWARE

8. PERFORMING ORGANIZATION REPORT NUMBER

9. SPONSORING/MONITORING AGENCY NAME(S) AND ADDRESS(ES)
THE DEPARTMENT OF THE AIR FORCE
AFIT/CIA, BLDG 125
2950 P STREET
WPAFB OH 45433

10. SPONSORING/MONITORING AGENCY REPORT NUMBER
FY00-186

11. SUPPLEMENTARY NOTES

12a. DISTRIBUTION AVAILABILITY STATEMENT
Unlimited distribution
In Accordance With AFI 35-205/AFIT Sup 1

12b. DISTRIBUTION CODE

13. ABSTRACT *(Maximum 200 words)*

14. SUBJECT TERMS

15. NUMBER OF PAGES
90

16. PRICE CODE

17. SECURITY CLASSIFICATION OF REPORT	18. SECURITY CLASSIFICATION OF THIS PAGE	19. SECURITY CLASSIFICATION OF ABSTRACT	20. LIMITATION OF ABSTRACT

STRUCTURES AND CHEMISTRY OF AMINO AND NITRO FURAZANS

by

Royce W. Beal

Approved: Thomas B. Brill

Thomas B. Brill, Ph.D.
Professor in charge of thesis on behalf of the Advisory Committee

Approved: Steven D. Brown

Steven D. Brown, Ph.D.
Chair of the Department of Chemistry and Biochemistry

Approved: _____

Conrado M. Gempesaw, II, Ph.D.
Vice Provost for Academic Programs and Planning

ACKNOWLEDGMENTS

I am grateful to the Civilian Institutions Section of the Air Force Institute of Technology of the United States Air Force for the opportunity to advance my education and knowledge as well as the financial support required to do so.

I am also grateful for the help, support, and knowledge provided to me by the Faculty and Staff of the Department of Chemistry at the University of Delaware with specific thanks to my mentor, Dr. Thomas B. Brill for his dedication to learning and his academic excellence. For their insight, help, and friendship, I thank also the members of the Brill research group. I have very much appreciated the advice and service of Dr. Douglas Doren and Dr. Arnold Rheingold and their respective research groups.

I thank my parents for teaching me how to learn and grow and how to explore my insatiable curiosity in productive ways. I thank my wife Christina, for her unconditional love and support and for constantly inspiring me to succeed. I thank my son Leo, for reminding me how fundamentally important learning really is.

I humbly express my gratitude to my creator for the charity He has shown unto me.

TABLE OF CONTENTS

LIST OF TABLES

LIST OF FIGURES

ABSTRACT

The furazan ring has become the subject of significant investigation in recent years due to its potential as a ballistic modifier and fuel in energetic materials formulations. This thesis is a study of compounds with amino and nitro substitution on one or two furazan rings. Dinitrogen groups are the bridge for the two-ring systems. The synthesis and characterization of these compounds is presented. Dinitrohydrazofurazan is a new compound. Flash-pyrolysis by T-Jump/FTIR spectroscopy was performed on these compounds to determine the pyrolysis products. X-ray crystallography was performed on five compounds and structural details are compared. Density functional theory calculations were performed on all of the compounds to compare the heats of formation and establish the atom motions that most dominate the IR absorptions.

CHAPTER 1

INTRODUCTION

1.1 Background and Purpose

Technological advances have been made. Old problems are being reinvestigated by new methods. In the case of the exhaust from solid rocket propellants, observability and to some degree toxicity have proven to be a liability of conventional formulations. Much of both problems stems from the metallic ingredients used as fuels and combustion modifiers. Replacement of these ingredients with compounds that yield only non-toxic, invisible gases such as N_2 upon combustion has been pursued as a possible solution. Thus a significant insurgence of interest in high nitrogen compounds as additives or ingredients in energetic mixtures has occurred in recent years.

An important category of high-nitrogen compounds involves the furazan ring

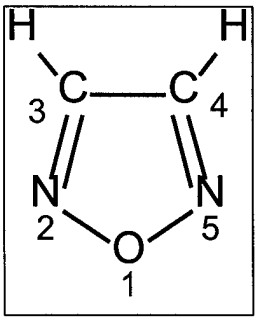

whose IUPAC name is 1,2,5-oxadiazole. The furazan ring shown below has drawn attention as one of several stable backbone structures that can be easily functionalized by substitution at each carbon atom. However, an oxygen atom can datively bond to one of the nitrogen atoms giving rise to the furoxan ring. Metal atoms can

also coordinate to the nitrogen. Neither the furoxan structure nor metal complexes are the subject of the present work.

Depending on the electron withdrawing and donating substituents in the 3 and 4 positions, a wide array of compounds can be derived. These compounds range from relatively inert to extremely sensitive in terms of their response to heat and impact. Furthermore, furazan rings can be linked together either directly or with a functional group bridge thus allowing for a replication of the ring structure and construction of higher molecular weight "oligomers" and macrocycles.

Compounds based on the furazan ring have attractive properties as organic energetic materials. First, the aromaticity of the ring stabilizes the backbone. Secondly, the resulting planarity of the ring permits better crystal packing resulting in high density. Third, the oxygen atom in the ring is not bonded to either carbon or hydrogen and is able to engage in redox chemistry when bonding to carbon in the eventual decomposition products. Partly for these reasons, compounds based on the furazan ring have been heavily investigated in large part by the energetic materials community.

While formulating new solid rocket propellants, it has been discovered that selected furazan compounds affect the burning rate and pressure exponent of propellants when added in small amounts (usually less than 10%). The application of most furazan compounds has been limited however by their lack of availability in a production scale. This fact not withstanding, furazan compounds still have the potential to modify combustion behavior while adding significantly to the energetic yield of the propellant formulation. Therefore, interest in them remains high, especially in the US and Russia.

The first reference to furazan-derived compounds with an obvious emphasis on their energetic potential was published first over thirty years ago in the US. The next major reference came from Russia in 1980. However, not until the late 1980's did the significant interest in furazans become evident in the open literature. In 1994, a review article on the nitration of aminofurazans originated from Russia. This review article, which is now widely referenced in articles related to this subject, contained exhaustive work, which had only recently been declassified. Since this review several articles have been published from US and Russian sources each year on topics ranging from basic chemical research to specific engineering applications. The following is a brief review of the furazan field to the present.

Wolff[1] first mentioned furazan synthesis in 1895 via a condensation of glyoxime. In 1968, Coburn[2] reported the synthesis of substituted furazans and bifurazans via a ring closure of the corresponding substituted glyoxymes. Specifically mentioned were picryl substituents and nitration of amino substituents subsequent to ring formation. The motivation of this primarily synthetic effort was the consideration and evaluation of the resulting compounds as high explosives. No further reference was found to this class of compounds as energetic materials until the high densities and high heats of formation were predicted in the early 1980s.[3,4]

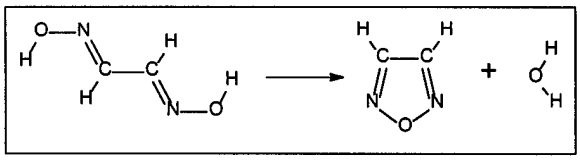

In the 1980's, Solodyuk[5] reported an oxidation of 3,4-diaminofurazan to 3-amino-4-nitrofurazan via peroxide reagents. This paper also suggested a stepwise oxidation of

the amino group through the hydroxylamino-, then nitroso-, and finally nitro- group. This set of intermediates was used to suggest a scheme that accounted for the production of the 4,4'-diaminoazofurazan and the 4,4'-diaminoazoxyfurazan during the same reaction that yielded the aminonitrofurazan.

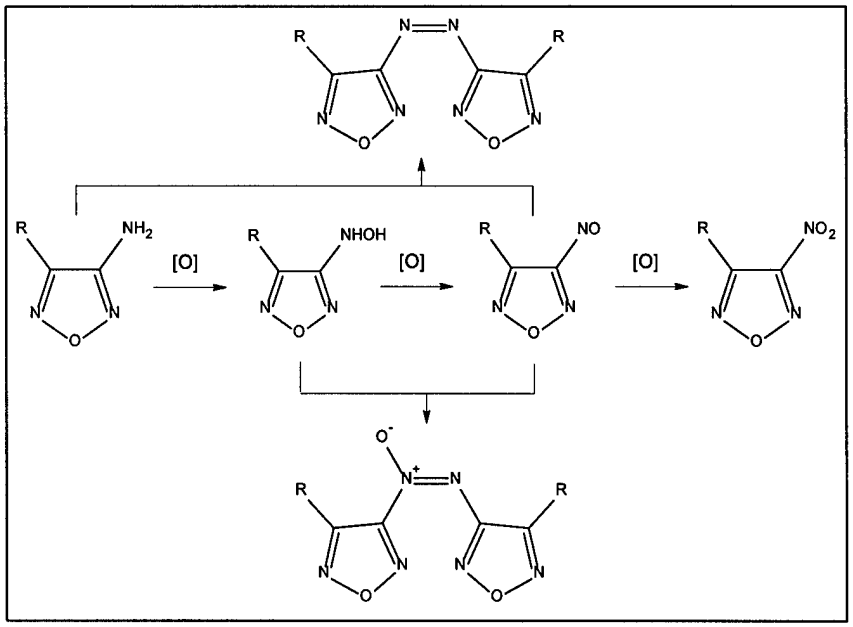

Acting on the aforementioned prediction of their usefulness in the energetic materials community, Oyumi and Brill[6] reported on the thermal decomposition of a furazan derivative in 1986. In this case the substituents were cyclic thus forming a heterocycle. However, X-ray crystallographic data of the compound were reported and clearly showed the planarity of the furazan ring.

Several more Russian papers appeared between 1986 and 1989. One dealt with furazan-metal complex interactions[7]. Another dealt with some pyrolysis of the furazan and furoxan rings and suggested a mechanism by which the furazan ring decomposes.[8] Yet another described the reactions of the azoxy-bridging moiety in furazan compounds with nucleophiles yielding single ring compounds.[9] Collectively these papers showed

that Russian workers were actively pursuing an understanding of both the furazan ring and it derivatives for years.

In 1990, Chi, et al.,[10] patented the use of diaminofurazan (DAF) as a ballistic modifier in ammonium perchlorate based composite propellants. Shortly thereafter, Stoner and Brill[11] published the results of a thermal decomposition study of diaminofurazan. They suggested that diaminofurazan can decompose into compounds, which can further react to form melamine-like cyclic azines. It was previously known that ammonia suppressed the burning rate of ammonium perchlorate based propellants and this study further demonstrated that ammonia is formed during the decomposition of DAF. These reactions were offered to explain the effect of DAF on the combustion characteristics of composite rocket propellants. That same year Stoner and Brill[12] published a paper reporting on the thermal decomposition of copper (II) complexes of DAF. This study predicted that the metal complexes of these compounds would not affect burning rates in the same way as the parent DAF molecule. Also in 1990, Sheremetev[13] reported on the synthesis of nitrosofurazans via peroxides, sulfuric acid, and ammonium persulfate. This work was very reminiscent of that of Solodyuk nearly ten years earlier and in fact reported the finding of the azoxy- bridging as Solodyuk had.

In 1993, a new synthetic effort in the US was introduced by Boyer, et al. [14] This paper referenced the 1968 Colburn work as well as the 1980 Solodyuk work. Furthermore, the motivation was the pursuit of organic energetic materials. This paper also described a synthesis for DAF in good yield and is referenced and repeated in most subsequent work dealing with furazans.

Sheremetev's[15] 1994 paper outlined a general preparation of nitrofurazans using various oxidizing media based primarily on hydrogen peroxide, but also used sulfuric acid, ammonium persulfate, and sodium tungstate. It was proposed that each aminofurazan compound had a threshold ionization potential which corresponded to an active oxygen factor. A table was published with 33 aminofurazans and their ionization potentials. Additionally, a curve was given by which the ionization potentials were related to the active oxygen factors and a table was provided which correlated a series of reagents and ratios thereof to their active oxygen factor. Using these tables, one could theoretically establish the active oxygen requirement for any aminofurazan oxidation to the nitro analog and find an appropriate set of reagents which would meet that requirement. While subsequent synthetic work has varied somewhat in choice of oxidizing agents, nearly all oxidations of aminofurazans use this general scheme and nearly all synthetic papers dealing with furazans thereafter reference this paper. Furthermore, the potential of the intermediates of these oxidation reactions to bridge the rings as demonstrated by Solodyuk has been employed to make multiple ring oligomers based on the compounds in Sheremetev's paper.

In that same year Brill, et al., published two more papers built upon his earlier work. One investigated other high nitrogen compounds that might form melon-like azines in an effort to find other ballistic modifiers.[16] The other investigated the kinetics of the decomposition of the furazan containing heterocycle that they previously investigated in 1986.[17]

Also in 1994, Boyer[18] published another synthetic effort describing nitro and azido substitutions of the furazan, furoxan, and two ring systems. In addition to the several compounds reported for the first time in this paper, he indicated that DAF could be purchased from Sigma-Aldrich. This commercial availability further demonstrated the growing interest in compounds using DAF as a starting material. At the same time, Kulagina[19] reported the synthesis of fully nitrated compounds containing two, three, and four furazan moieties. Although the azoxy bridge was of particular interest in this paper, some azo bridges were reported. Epishina[20] reported on the synthesis of macrocycles based on diaminobifurazan. These contained four, six, and eight furazan rings.

As interest in furazan compounds has grown, so has the need for cheaper starting materials. In 1995, Trudell[21] reported a new synthesis of diaminoglyoxime that was simpler and cheaper than the previously used methods. At the same time, Sheremetev[22] published several important synthetic routes to bridging functional groups, macrocycles, and nitration of aminofurazans.

In 1996, Batog, et al., published two papers on the macrocyclization of

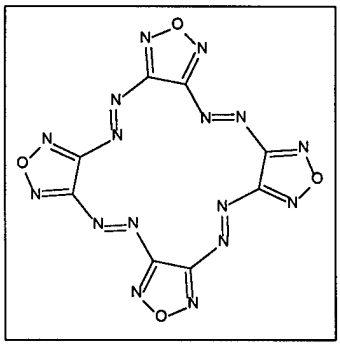

diaminoazofurazan. The first reported the synthesis of macrocycles containing 3, 4, 5, 6, and 8 furazan moieties, all bridged with an azo group.[23] The second paper discussed the synthesis mechanisms and provided some new synthetic methods for the macrocycles, thus adding to the list of azo-linked macrocycles one containing only two furazan rings.[24]

Also in 1996, Sheremetev[25] reported the synthesis of several high energy compounds. In that paper, he outlined the most promising synthetic pathways he had been working with and furnished significant characterization of these compounds. A database on relations between structure and physical properties was made.

Between 1997 and the present, at least six groups have been actively researching furazan chemistry. Sheremetev[26] published another paper dealing with synthesis recounting most of the synthetic schemes in use. It emphasized the construction of oxy, azo, and azoxy bridging functionalities. One scheme of major significance was the use of potassium permanganate to oxidatively couple amino groups giving rise to an azo bridge. This paper also reported some physical properties of thirty compounds.

Sheremetev, Sinditskii, and Fogelzang[27] focussed on combustion and combustion mechanisms of the high energy furazan-based compounds. The burning rate data were given for several of the compounds, which seem to be the most promising for application as propellant ingredients. Comparisons were made between diamino compounds with different bridges. Also compounds were compared with the same bridging moiety but differing substituents. It was concluded that the majority of the energy release from the decomposition of the furazan ring came not from redox chemistry involving the oxygen atom but rather isomerization and partial fragmentation. The other paper focused on the decomposition of DAF.[28] Its burning rate was studied as was the combustion mechanism and flame structure. As suggested by Stoner and Brill previously, substantial residue was found upon combustion of DAF and an attempt was made to characterize this residue. The conclusions confirm the work of Brill.

Batog, et al., continued to work on synthesis macrocycles containing the furazan ring. One paper on this topic introduced methods to convert the azo bridge to an azoxy bridge in an existing macrocycle[29]. A structure derived from x-ray crystallography of a four furazan membered macrocycle with azoxy bridges was given along with other characterization data. Another paper reviewed the macrocyclization reactions of furazans.[30] It presented the established synthetic schemes and offers some physical data of some of the more common of the macrocycles.

Williams and Brill[31] published a paper during this time on the flash pyrolysis of six furazan containing compounds. However, four of these were salts were previously unknown. Specifically, they were the ammonium, hydrazinium, hydroxylammonium, and sodium salts of nitraminonitrofurazan. Nitraminonitrofurazan and aminonitrofurazan were included. The products of decomposition were quantified and listed. Furthermore, some kinetics were determined and the decomposition mechanisms were discussed. Although the conclusions were that the initial step in the decomposition depended upon the substituent, the suggestion was made that initial N-O bond cleavage occurs in compounds having relatively stable substituents. An apparent activation energy was determined.

Trudell, et al., also published two papers since 1997. The first dealt extensively with synthetic procedures and characterization of aminonitroazoxyfurazan.[32] X-ray crystallographic data and fairly complete characterization data were given for the parent compound. The second paper similarly described dinitroazofurazan.[33] Again x-ray crystallography was performed on the parent compound.

The Thiokol Corporation had investigated these compounds prior to 1997, but their results only became available recently.[34] As a company that develops solid rocket motors, their interest in furazan chemistry is obvious and much of the work was internally funded. Some of the work was conducted under contract to the US Air Force. The work coming from Thiokol was significant because more economical and more efficient synthetic routes to many of the more promising compounds were pursued. Also, various of the furazan compounds were tested for compatibility with other rocket propellant ingredients in order to narrow the scope of investigation to only those that could potentially be useful.

For many of the same reasons that Thiokol became interested in furazans, the High Explosives Science and Technology group at Los Alamos National Laboratory began investigating the combustion and explosive properties of several furazan compounds. Burning rate measurements were published as well as detonation velocities for various densities of different compounds.[35] One of the papers from Los Alamos offered a novel approach to synthesize diaminoazofurazan by reducing the diaminoazoxyfurazan to the diaminohydrazofurazan and then slowly oxidizing this to get the target compound.[36] The hydrazo linkage had not previously been considered in the literature and the diaminohydrazofurazan mentioned in their synthesis is a compound novel to the work at Los Alamos.

In summary, although the furazan ring has been known for more than one hundred years, its potential usefulness as an energetic material went unnoticed until 35 years ago. Only relatively recently has the chemistry begun to be studied at any significant level. In

this time, however, great strides have been made into understanding mechanisms and conditions of both its synthesis and decomposition. An understanding of how to obtain particular linking groups has been gained and this understanding has been used to make fairly large oligomers as well as macrocycles. It has been demonstrated that the furazan moiety can function as a ligand in metal complexes. It has also been shown that the diaminofurazan can suppress the burning rate of rocket propellants and other related compounds are suggested to behave similarly. Not discussed here is the fact that furazan-containing compounds have been considered for pharmaceutical uses. As an understanding of this chemistry grows, it is likely that more uses will be found.

This thesis focuses on systematically characterizing a closely related set of furazans shown in Table 1.1. The synthesis and flash pyrolysis of twelve furazan and difurazan compounds was attempted. These were the diamino-, aminonitro-, and dinitro-substitutions of four of the furazan ring systems, namely the single ring, the hydrazo-linked double ring, the azo-linked double ring, and the azoxy-linked double ring. Unfortunately, three of these compounds were never obtained for reasons that will be discussed.

Table 1.1 Compounds chosen for study in this thesis

(1) 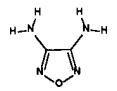 DAF diaminofurazan 3,4-diamino-1,2,5-oxadiazole	(2) 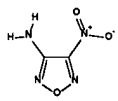 ANF aminonitrofurazan 3-amino-4-nitro-1,2,5-oxadiazole	(3) 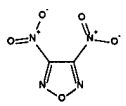 DNF dinitrofurazan 3,4-dinitro-1,2,5-oxadiazole
(4) 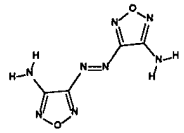 DAAzF diaminoazofurazan 4-[(4-amino-1,2,5-oxadiazol-3-yl)-NN-azyl]-3-amino-1,2,5-oxadiazole	(5) 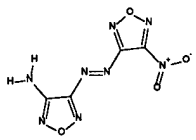 ANAzF aminonitroazofurazan 4-[(4-nitro-1,2,5-oxadiazol-3-yl)-NN-azyl]-3-amino-1,2,5-oxadiazole	(6) 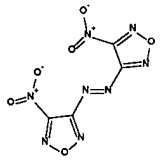 DNAzF dinitroazofurazan 4-[(4-nitro-1,2,5-oxadiazol-3-yl)-NN-azyl]-3-nitro-1,2,5-oxadiazole
(7) 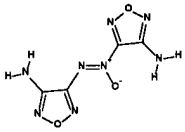 DAAF diaminoazoxyfurazan 4-[(4-amino-1,2,5-oxadiazol-3-yl)-NNO-azoxyl]-3-amino-1,2,5-oxadiazole	(8) 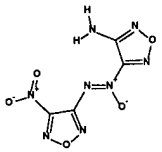 ANAF aminonitroazoxyfurazan 4-[(4-nitro-1,2,5-oxadiazol-3-yl)-NNO-azoxyl]-3-amino-1,2,5-oxadiazole	(9) 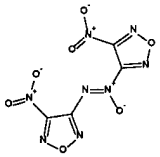 DNAF dinitroazoxyfurazan 4-[(4-nitro-1,2,5-oxadiazol-3-yl)-NNO-azoxyl]-3-nitro-1,2,5-oxadiazole
(10) 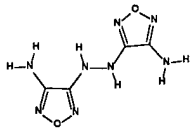 DAHzF diaminohydrazafurazan 4-[(4-amino-1,2,5-oxadiazol-3-yl)-NHNH hydrazyl]-3-amino-1,2,5-oxadiazole	(11) 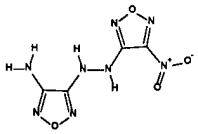 ANHzF aminonitrohydrazafurazan 4-[(4-nitro-1,2,5-oxadiazol-3-yl)-NHNH-hydrazyl]-3-amino-1,2,5-oxadiazole	(12) 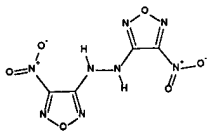 DNHzF dinitrohydrazafurazan 4-[(4-nitro-1,2,5-oxadiazol-3-yl)-NHNH-hydrazyl]-3-nitro-1,2,5-oxadiazole

Initially, this study was intended to focus on the physical characterization and flash pyrolysis of the target compounds. Samples of DAF were generously provided by the Air Force Research Laboratory and the Thiokol Corporation. Some synthetic work had already taken place at the Air Force Research Laboratory prior to the onset of this study and so they were able to provide some preparative instructions and literature references. Based on these instructions and the synthesis work in the literature, synthesis seemed to be straightforward. This was not the case and significant time was spent on synthesis work. As such, some of the difficulties encountered as well as the methods that eventually proved to be successful will be discussed. Eventually six of the compounds including one which is new to this field were synthesized. Three of the compounds were provided by other researchers and three were never obtained. Trudell[32,33] previously published x-ray crystallography results for two of the bicyclic systems. Attempts were made to grow crystals suitable for x-ray diffraction of the remaining bicyclic compounds that were obtained. These were moderately successful and the X-ray crystallographic data will be presented and discussed in chapter 4.

The decomposition studies of these compounds were carried out in an experimental apparatus designed for rapid and controlled heating and then observation of the gaseous products by rapid-scan FTIR spectroscopy. This experiment is referred to as T-Jump/FTIR spectroscopy. A small amount of the sample (the exact amount is unimportant as long as it is about 200 – 300 μg, because the results are based on ratios) is placed on a platinum ribbon heating filament, which in turn is placed inside an IR cell filled with an argon atmosphere. The pressure inside the cell can be made a variable

parameter of the experiment. The final filament temperature and rate of heating can also be varied as parameters of the experiment. The filament heating is triggered causing the material to decompose. As aerosol evaporate and gaseous products are generated, their IR spectra are observed and recorded by the FTIR spectrometer. The FTIR spectrometer takes data in a rapid scan mode at four scans per second. The design of the apparatus as well as specific parameters used will be discussed in Chapter 3.

High-level density functional theory calculations were performed on all twelve compounds. These were intended to provide the theoretical heat of formation for each compound because serious discrepancies exist in the values reported in the literature. The results of these calculations also provide insight in the atom motions responsible for the IR absorptions of these compounds and are given in chapter 5.

1.2 REFERENCES

1. Wolff, L., Chem. Ber., **28**, *69,* (1895).

2. Coburn, M. D., J. Heterocylic Chem., **5**, *83* (1968).

3. Rothstein, L. R. and Peterson, R., Propellants Explos., **4**, *56*, (1979).

4. Cichra, D. A.; Holden, J. R.; and Dickenson, C., NSWC Report TR79-273, Naval Surface Weapons Center, Silver Spring, MD, 1980.

5. Solodyuk, G. D.; Boldyrev, M. D.; Gidaspov, B. V.; and Nikolaev, V. D., Zhurnal Organicheskoi Khimii, **17**, *861* (1981).

6. Oyumi, Y.; Rheingold, A. L.; and Brill, T. B., J. Phys. Chem., **90**, *4686*, (1986).

7. Vasil'chenko, I. S.; Kochin, S. G.; Anisimova, V. A.; Khmel'nitskii, L. I.; and Garnovskii, A. D., Khim. Geterotsikl. Soedin., **5**, *666*, (1986).

8. Prokudin, V. G. and Nazin, G. M., Izv. Akad. Nauk SSSR, Ser. Khim., **1**, *221*, (1987).

9. Sheremetev, A. B.; Aleksandrova, N. S.; Novikova, T. S.; and Khmel'nitskii, L. I., Izv. Akad. Nauk SSSR, Ser. Khim., **3**, *749*, (1989).

10. Willer, R. L.; Chi, M.; Gleeson, B.; and Hill, J., Thiokol Corp., U. S. Patent 5071495, (1991).

11. Stoner, C. E. Jr. and Brill, T. B., Combust. Flame, **83**, *302*, (1991).

12. Stoner, C. E. Jr.; Rheingold, A. L.; and Brill, T. B., Inorg. Chem., **30**, *360*, (1991).

13. Sheremetev, A. B.; Novikova, T. S.; Mel'nikova, T. M.; and Khmel'nitskii, L. I., Izv. Akad. Nauk SSSR, Ser. Khim., **5**, *1193*, (1990).

14. Gunasekaran, A. and Boyer, J. H., Heterocycl. Chem., **4**, *521*, (1993).

15. Novikova, T. S.; Mel'nikova T. M.; Kharitonova, O. V.; Kulagina, V. O.; Aleksandrova, N. S.; Sheremetev, A. B.; Pivina, T. S.; Khmel'nitskii, L. I.; and Novikov, S. S., Mendeleev Commun., *138*, (1994).

16. Patil, D. G. and Brill, T. B., Thermochim. Acta, **235**, *225*, (1994).

17. Williams, G. K.; Palopoli, S. F.; and Brill, T. B., Combust. Flame, **98**, *197*, (1994).

18. Gunasekaran, A.; Trudell, M. L.; and Boyer, J. H., Heterocycl. Chem., **5**, *441*, (1994).

19. Kulagina, V. O.; Novikova, T. S.; and Khmel'nitskii, L. N., Chem. Heterocycl. Comp., **30**, *629* (1994).

20. Epishina, M. A.; Makhova, N. N.; Batog, L. V.; Konstantinova, L. S.; and Khmel'nitskii, L. I., Mendeleev Commun., *102*, (1994).

21. Gunasekaran, A.; Jayachandran, T.; Boyer, J. H.; and Trudell, M. L., J. Heterocycl. Chem., **32**, *1405*, (1995).

22. Sheremetev, A. B.; Kulagina, V. O.; Aleksandrova, N. S.; Novikova, T. S.; and Khmel'nitskii, L. I., Proc. Beijing Int. Symp. Pyrotech., *249,* (1995).

23. Eman, V. E.; Sukhanov, M. S.; Lebedev, O. V.; Batog, L. V.; Konstantinova, L. S.; Rozhkov, V. Y.; and Khmel'nitskii, L. I., Mendeleev Commun., *66*, (1996).

24. Batog, L. V.; Konstantinova, L. S.; Lebedev, O. V.; and Khmel'nitskii, L. I., Mendeleev Commun., *193*, (1996).

25. Sheremetev, A. B.; Kulagina, V. O.; Batog, L. V.; Lebedev, O. V.; Yudin, I. L; and Pivina, T. S., Proc. Int. Pyrotech. Seminar, 22nd, *377*, (1996).

26. Sheremetev, A. B.; Kulagina, V. O.; Aleksandrova, N. S.; Dmitriev, D. E.; Strelenko, Y. A.; Lebedev, V. P.; and Matyushin, Y. N., Prop. Explos. Pyrotech., **23**, *142* (1998).

27. Sinditskii, V. P.; Dong, H. W.; Serushkin, V.; Fogelzang, A. E.; and Sheremetev, A. B., Int. Ann. Conf. ICT, 29th (Energetic Materials), *170-1*, (1998).

28. Dong, H. W.; Sinditskii, V. P.; Serushkin, V. V.; Egorshev, V. Y.; and Fogelzang, A. E., Int. Pyrotech. Seminar, 26th, Nanjing, China, October 1-4 (1999).

29. Eman, V. E.; Sukhanov, M. S.; Lebedev, O. V.; Batog, L. V.; Konstantinova, L. S.; Rozhkov, V. Y.; Dekaprilevich, M. O.; Struchkov, Y. T; and Khmel'nitskii, L. I., Mendeleev Commun., *5*, (1997).

30. Batog, L. V.; Konstantinova, L. S.; Rozhkov, V. Y.; Lebedev, O. V.; Epishina, M. A.; Makhova, N. N.; Ovchinnikov, I. V.; and Khmel'nitskii, L. I., Int. Ann. Conf. ICT, 29th, *P55*, (1998).

31. Williams, G. K. and Brill, T. B., Combust. Flame, **114**, *569,* (1998).

32. Zelenin, A. K.; Stevens, E. D.; and Trudell, M. L., Struct. Chem., **8**, *373,* (1997).

33. Zelenin, A. K.; Trudell, M. L.; and Gilardi, R. D., J. Heterocyclic Chem., **35**, *151* (1998).

34. Lou Cannizzo, Thiokol Corp., Brigham City, UT, Personal Communication (1999).

35. Son, S. F.; Berghout, H. L.; Bolme, C. A.; Chavez, D. E.; Naud, D.; and Hiskey, M. A., 1999 JANNAF PSHS Meeting, Cocoa Beach, FL, October 18-22, (1999).

36. Chavez, D.; Hill, L.; Hiskey, M.; and Kinkead, S., J. Energet. Mat., (1999) in press.

CHAPTER 2

SYNTHESIS AND CHARACTERIZATION

The synthesis of aminated and nitrated furazan derivatives has been the focus of much of the reported research into furazan chemistry in recent years. The research in this thesis necessitated the synthesis and characterization of most of these compounds, although a few could be acquired from other researchers. Table 1.1 gave the compounds of interest.

2.1 DAF

Two 25 g samples of DAF were donated; one by the Thiokol Corporation, Elkton MD, and the other by the Air Force Research Laboratory, Edwards AFB, CA. The material provided by Thiokol was primarily used in later synthesis. DSC was performed on this material and showed an onset for melting at 180°C (lit: 180°C)[1] and an onset for exothermic decomposition at 241°C.

2.2 ANF

ANF has been synthesized previously[2] and was repeated as follows: A 100 ml 3-neck flask was placed in an ice bath with stirring. An addition funnel was attached to one

neck of the flask. A 50% H_2O_2 (55.89 ml, 0.969 mol) solution was added to the flask and 8.44 ml of a 96% H_2SO_4 (0.152 mol) solution was added to the funnel. When the temperature of the peroxide solution was under 5°C, the addition of the acid was begun taking care to not let the temperature rise above 5°C. When the addition was complete, $Na_2WO_4(2H_2O)$ (4.71 g, 0.0143 mol) was added all at once. Thereafter, DAF (1) (1.10 g, 0.011 mol) was added little by little to prevent the temperature from rising above 5°C. Upon completion of this addition, the reaction was brought to room temperature and stirred for 18 hours. The resulting yellow solution was treated with Na_2CO_3 until the pH was at or near neutral. The solution was then filtered. The filtrate solution was extracted with CH_2Cl_2 three times and the extracts were combined and dried over anhydrous $MgSO_4$. The solvent was then removed by a rotovap leaving bright yellow crystals. These crystals were dissolved in a minimum of hot $CHCl_3$ and the solution carefully transferred to a beaker. This solution was cooled in a refrigerator yielding needle-like yellow crystals which had a DSC melting onset of 120°C (lit: 122-125°C) [3] and an onset of exothermic decomposition of 170°C. The infrared spectrum matched the literature[3] very well. X-ray crystallography confirmed that the crystals were ANF.

2.3 DNF

Two attempts were made to synthesize DNF. These were based on the only preparation of this compound described in the literature[2] which indicated the need for a 2:1:0.05 mole ratio of 93% H_2O_2:conc. H_2SO_4:Na_2WO_4. The amount of aminofurazan reactant to be nitrated was not indicated. The H_2O_2 used was prepared by concentrating

commercially available 30% H_2O_2 on a rotovap and was determined by density to be about 90%. In the first attempt, 8.43 ml of the H_2O_2 solution was placed in a three neck flask with stirring and cooled to 0°C. To this was added 8.70 ml of conc. H_2SO_4 dropwise, never letting the temperature exceed 5°C. To this was added the Na_2WO_4 all at once resulting in a violent and highly exothermic reaction. This was immediately quenched with water and discarded. The second attempt used the same amounts of material but the H_2O_2 solution was cooled to –20°C. This froze the solution and the H_2SO_4 was added to this. The Na_2WO_4 was then added and the mixture was allowed to warm slowly to 0°C. The resulting solution was stable at 0°C. To this was added 0.813 g ANF and the solution was allowed to come to room temperature and stir for 1 hour. The resulting solution was extracted with CH_2Cl_2 and the extract rotovaped to the persistence of a very small amount of liquid. This liquid was found to be mostly water. No further attempts at synthesis were made.

2.4 DAAzF

The following describes a successful synthesis of DAAzF based on a reported procedure.[4] A 250 ml Erlenmeyer flask was charged with 67 ml H_2O and to this was added $(NH_4)_2S_2O_8$ (52.03 g, 0.23 mol). The solution was heated to 50°C with stirring. Thereafter, DAF (1) (4.17 g, 0.042 mol) was added yielding a yellow color right away which began to darken. The mixture was then heated to 70°C and held there for 2 hours. At the end of this time, yellow solids had begun to form and separate from the solution. The mixture was filtered and the solids collected were washed with warm H_2O and then

dried. These solids were then soxhlet extracted using THF as the solvent. The extract was rotovaped leaving a yellow solid that had a DSC profile that was nearly identical to pure DAAF (7). The solids remaining in the extractor were dissolved into CH_3CN/DMSO (3:1) and then precipitated with addition of H_2O. This precipitate was filtered and dried to leave reasonably pure DAAzF, which showed a decomposition onset by DSC of 310°C and peak at 317°C (lit: 325 decomp.).[3] Infrared spectra matched the literature spectrum[3] as well.

2.5 ANAzF

Several attempts were made to synthesize ANAzF. The first few attempts were made based on the 1994 Sheremetev paper.[2] The general procedure in this paper is to cool H_2O_2 to 0°C and slowly add H_2SO_4 and finally another, usually solid, oxidizing agent if called for. Ratios and concentrations are derived via a series of tables. Several of these combinations were attempted. H_2O_2 (30%), H_2SO_4, and $(NH_4)_2S_2O_8$ in a mole ratio of 2:1:0.5 yielded starting material. H_2O_2 (50%) and H_2SO_4, in a mole ratio of 2:1 yielded starting material. H_2O_2 (50%), H_2SO_4, and $(NH_4)_2S_2O_8$ in a mole ratio of 2:1:0.2 yielded starting material.

The next idea was to reduce a nitro group to an amino group in DNAzF (6) using Fe and acetic acid in ethanol. This was based on a reference[5] indicating the possibility of selective reduction of one out of two nitro groups. This resulted in the synthesis of the previously unknown DNHzF (12) and specific synthetic details are given later. Similar reduction based on S^{2-} failed to yield anything recognizable as a furazan adduct. Another

idea was based on linking DAF (1) and ANF (2) using $KMnO_4$ based on the synthesis of DNAzF (6) which oxidatively links the amino groups in ANF (2). This attempt resulted in impure DNAzF (6). The next idea was to reduce the azoxy (-N(O)=N-) linkage in ANAF (8) to an azo linkage based on the reduction of the azo linkage to the hydrazo linkage observed in the synthesis of DNHzF (12) as mentioned above. Attempts at this were carried out in various combinations of conditions. The solvents used were ethanol and CH_2Cl_2. Zn powder as well as Fe wire was used as reducing agents and various times and temperatures were attempted. These yielded either starting material or DAAzF (4) depending mostly on temperature. No further synthesis attempts were made.

2.6 DNAzF

The following describes a successful synthesis of DNAzF by the reported procedure.[6] In a 250 ml round bottom flask, ANF (2) (0.40 g, 3.1 mmol) was dissolved in 16 ml of concentrated HCl (0.53 mol) with stirring. $KMnO_4$ (0.95 g, 6.0 mmol) was dissolved in 106 ml H_2O and placed in a dropping funnel which was in turn affixed to the round bottom flask. The acid solution was heated to 40°C and the $KMnO_4$ solution was added over the period of an hour. The resulting dark brown/black solution was heated to 55-60°C for 2 hours with continued stirring. The solution was then allowed to cool to room temperature whereupon it was extracted with 4 x 50 ml aliquots of CH_2Cl_2. The extracts were combined and washed twice with H_2O. The organic phase was then dried with anhydrous $MgSO_4$ and filtered. The remaining solution was rotovaped until only an orange oil remained. The oil appeared to be DNAzF by IR, but would not crystallize

even after several days in the freezer. It was dissolved in pentane/CH_2Cl_2 (1:2 by volume) and passed through a small amount of silica gel. The resulting solution was once again dried and once again crystals failed to form. Eventually, small (2 ml) portions of benzene were added and rotovaped off. This was done three times in an effort to remove H_2O. After two days in the freezer, the oil had completely crystallized and had a DSC melting onset of 48°C (lit: 56°C)[6] and a peak of 55°C. It is interesting to note that on subsequent attempts to synthesize this material, no particular effort was expended or required to promote crystal growth and indeed on the third and final run of this procedure cooling was not even necessary.

2.7 DAAF

The following describes a successful synthesis of DAAF by the literature method.[2] A 250 ml 3-neck flask was charged with 36.8 g (0.325 mol) of 30% aqueous solution of H_2O_2. To this was added 3.678 g (0.0368 mol) DAF (1) all at once. The flask was placed in a temperature control bath and was fitted with an addition funnel. As the suspension was cooled to below 20°C, the funnel was charged with 20.23 g (0.198 mol) of a 96% solution of H_2SO_4. When the suspension was below 20°C, addition of the acid was begun at a rate, which would not allow the temperature to rise above 25°C. Upon completion of the addition, the suspension was allowed to come to room temperature and stir for 18 hours. The yellow solids were collected on a glass frit and rinsed with cold water twice. The solids were dried under vacuum. These crude solids were eventually purified by recrystallization. They were dissolved a minimum of N,N-

dimethylformamide. To this solution was added water causing a yellow precipitate, which was filtered and rinsed with cold water. This was done twice to yield material with a DSC exothermic decomposition onset of 249°C (lit[3]: 249°C melt). The material also fit the literature[3] infrared spectrum very well. Crystals of this material were grown out of DMF and H_2O and were shown by X-ray crystallography to be DAAF.

2.8 ANAF

A 5 g sample of ANAF was provide by the Air Force Research Laboratory. This material was the raw material from a synthesis attempt and was reported to be very impure. Thin layer chromatography (TLC) was performed on the sample using hexanes/THF (7:3 by volume). The TLC showed at least four spots thus confirming the report of significant impurity. Efforts at separation by column chromatography using the same solvent failed. Use of preparation thin layer chromatography provided material with only two spots in TLC. A sample of the material was dissolved in a minimum of DMSO and water was added to this. Immediately a yellow precipitate was observed. This material showed only one spot in TLC and melted at 128°C. Eventually, all of the material provided was dissolved in DMSO and water was slowly introduced by vapor diffusion. This yielded large orange/red crystals, which had a DSC onset of melting at 125°C (lit: 131°C)[3] and an onset of exothermic decomposition at 160°C. The infrared spectrum fit the literature spectrum[7] very well. X-ray crystallography was performed and showed the crystals to be ANAF.

2.9 DNAF

The following describes a successful synthesis of DNAF by the literature method.[4] A 125 ml Erlenmeyer flask was charged with 15 ml of 30% H_2O_2 (0.49 mol). This was placed in an ice bath on a stir plate and a stir bar was placed in the flask. To the flask was then added $(NH_4)_2S_2O_8$ (11.97 g, 0.053 mol). The solution was stirred and allowed to cool. Separately, a 50 ml beaker was charged with 12.5 ml of 96% H_2SO_4 (0.23 mol) and to this was added DAAF (7) (1.06 g, 0.005 mol). The beaker was warmed and stirred by hand until the DAAF (7) dissolved into the acid. The acid solution was then pipetted into the Erlenmeyer flask little by little to prevent the solution from exceeding 20°C. This solution was then stirred overnight. The resulting solution was washed into a 250 ml Erlenmeyer containing 100 ml ice cold water with cold water. This was filtered and the filtrant collected and dissolved into about 50 ml of CH_2Cl_2. This solution was washed with 2 aliquots of about 10 ml of a saturated solution of $NaHCO_3$. It was then washed once more with about 10 ml of water. These were each in turn separated from the solution using a separating funnel. The solution was passed through a small amount of silica gel and left to evaporate in a fume hood. After 2 days large bright yellow crystals remained. These were found by X-ray crystallography to be DNAF and had DSC onset of melting at 108°C (lit: 110-112°C)[8] and an onset of exothermic decomposition at 206°C. The infrared spectrum fits the literature spectrum[8] very well.

2.10 DAHzF

A 500 mg sample of DAHzF was provided by Los Alamos National Laboratory. DSC was performed on this material and showed an onset of melting at 188°C which was followed closely by a mild exotherm. Curiously, in a few attempts the material proceeded into the mild exotherm without ever showing the endotherm attributed to melting. In all cases, a strong exothermic decomposition was observed with an onset of 312°C. As will be discussed later, this exotherm is attributed to the decomposition of DAAzF (4).

2.11 ANHzF

As ANAzF (5) was considered the only practical starting material for a synthesis of ANHzF, no attempt was made to synthesize this material.

2.12 DNHzF

The following describes a successful synthesis of DNHzF. To about 25 ml of ethanol in a 100 ml round bottom flask, glacial acetic acid (0.013 g, 0.22 mmol) was added. To this was added DNAzF (6) (0.050 g, 0.20 mmol) as well as about 0.5 g Fe wire. This was stirred and refluxed for about an hour. Thereafter, about 25 ml H_2O was added as well as about 1 g $NaHCO_3$. This was extracted with 3 x 20 ml aliquots of CH_2Cl_2. The extracts were combined and washed twice with H_2O. The resulting solution was then dried with anhydrous $MgSO_4$ and filtered. The solvent was removed to yield yellow crystals that had a DSC onset of melting at 160°C and a peak of 171°C. The DSC

also showed an onset to an exothermic decomposition at about 200°C and two peaks, one at 215°C and the other at 227°C. IR, MS and X-ray crystallography showed the compound to be DNHzF. Incidentally, this procedure was originally intended to reduce a nitro group on the parent compound in an effort to synthesize ANAzF (5). This attempt yielded instead DNHzF, which to our knowledge is previously unknown. Later synthesis of this compound used Zn powder in place of Fe wire with similar results.

2.13 Summary

In most cases, characterization rested heavily on DSC profiles and IR spectra. X-ray crystallography was performed when possible and verified the identity of the compounds for which they were run. Table 2.1 gives some characterization data. Table 2.2 gives some of the more prominent or identifying absorbances in the IR spectra.

Table 2.1 Physical characteristics of target compounds

Name	Abbreviation	#	Formula	ρ (g/cm^3) (crystal)	ρ (g/cm^3) (lit.)	ox. bal. (CO_2)	ox. bal. (CO)	m.p.	dec.	ΔH_f (Kcal/mol)
Diaminofurazan	DAF	1	$C_2N_4H_4O$	-	1.61 [9]	-79.94%	-47.96%	180	240	25 [10]
Aminonitrofurazan	ANF	2	$C_2N_4H_2O_3$	-	1.86 [9]	-24.61%	0.00%	125	170	27 [10]
Dinitrofurazan	DNF	3	$C_2N_4O_5$	-	1.62 [2]	10.00%	29.99%	-15	220	
Diaminoazofurazan	DAAzF	4	$C_4N_8H_4O_2$	1.77	1.73 [4]	-65.27%	-32.64%	305	305	128 [11]
Aminonitroazofurazan	ANAzF	5	$C_4N_8H_2O_4$	-	-	-35.38%	-7.08%	93	N/A	
Dinitroazofurazan	DNAzF	6	$C_4N_8O_6$	1.74 [12]	1.73 [9]	-12.50%	12.50%	56	210	168 [10]
Diaminoazoxyfurazan	DAAF	7	$C_4N_8H_4O_3$	1.76	1.75 [11]	-52.80%	-22.63%	249	249	106 [11]
Aminonitroazoxyfurazan	ANAF	8	$C_4N_8H_2O_5$	1.86 [13] *	-	-26.44%	0.00%	131	160	
Dinitroazoxyfurazan	DNAF	9	$C_4N_8O_7$	1.84	1.82 [9]	-5.88%	17.64%	110	206	155 [10]
Diaminohydrazofurazan	DAHzF	10	$C_4N_8H_6O_2$	1.63 *	-	-72.69%	-40.38%	187	193	50 [11]
Aminonitrohydrazofurazan	ANHzF	11	$C_4N_8H_4O_4$	-	-	-42.09%	-14.03%	N/A	N/A	
Dinitrohydrazofurazan	DNHzF	12	$C_4N_8H_2O_6$	1.79	-	-18.60%	6.20%	165	200	

* Crystal latice contains solvent

Table 2.2 Infrared spectra of target compounds

Abbreviation	#	Formula	Prominent IR absorbances (cm^{-1})							
DAF	1	$C_2N_4H_4O$	3435 s	3321 s	3261 s	1646 s	1589 s	1475 m	1352 m	860 w
ANF	2	$C_2N_4H_2O_3$	3471 s	3448 s	3340 s	1639 s	1524 s	1371 vs	1043 m	832 vs
DNF	3	$C_2N_4O_5$	-							
DAAzF	4	$C_4N_8H_4O_2$	3444 s	3335 s	1640 s	1622 s	1498 m	1421m	1038 m	799 m
ANAzF	5	$C_4N_8H_2O_4$	-							
DNAzF	6	$C_4N_8O_6$	1572 s	1535 m	1446 w	1348 m	1178 m	1029 m	914 m	821 s
DAAF	7	$C_4N_8H_4O_3$	3429 s	3331 s	1637 vs	1510 m	1406 s	1348 m	1020 s	772 m
ANAF	8	$C_4N_8H_2O_5$	3460 s	3331 s	1637 vs	1577 vs	1407 m	1351 s	1162 m	834 s
DNAF	9	$C_4N_8O_7$	1575 s	1517 m	1409 m	1349 m	1315 m	1129 m	1035 m	819 s
DAHzF	10	$C_4N_8H_6O_2$	3398 s	3328 s	3219 vs	3041 s	1648 s	1439 m	1293 m	816 m
ANHzF	11	$C_4N_8H_4O_4$	-							
DNHzF	12	$C_4N_8H_2O_6$	3369 m	1623 vs	1529 s	1442 m	1394 m	1345 m	1192 m	837 s

2.14 References

1. Coburn, M. D., J. Heterocyl. Chem., **5**, *83* (1968).

2. Novikova, T. S.; Mel'nikova T. M.; Kharitonova, O. V.; Kulagina, V. O.; Aleksandrova, N. S.; Sheremetev, A. B.; Pivina, T. S.; Khmel'nitskii, L. I.; and Novikov, S. S., Mendeleev Commun., *138*, (1994).

3. Solodyuk, G. D.; Boldyrev, M. D.; Gidaspov, B. V.; and Nikolaev, V. D., Zhurnal Organicheskoi Khimii, **17**, *861* (1981).

4. Lou Cannizzo, Thiokol Corp., Brigham City, UT, Personal Communication, (1999).

5. Wulfman, D. S. and Cooper C. F., Synthesis, *924* (1978).

6. Zelenin, A. K. and Trudell, M. L., J. Heterocycl. Chem., **35**, *151* (1998).

7. Zelenin, A. K.; Stevens, E. D.; and Trudell, M. L., Struct. Chem., **8**, *373* (1997).

8. Gunasekaran, A.; Trudell, M. L.; and Boyer, J. H., Heteroatom Chem., **5**, *441*, (1994).

9. Sheremetev, A. B.; Kulagina, V. O.; Aleksandrova, N. S.; Dmitriev, D. E.; Strelenko, Y. A.; Lebedev, V. P.; and Matyushin, Y. N., Prop., Explos., Pyrotech., **23**, *142* (1998).

10. Sinditskii, V. P.; Dong, H. W.; Serushkin, V.; Fogelzang, A. E.; and Sheremetev, A. B., Int. Ann. Conf. ICT, 29th (Energetic Materials), *170-1*, (1998).

11. Chavez, D.; Hill, L.; Hiskey, M.; and Kinkead, S., J. Energet. Mat., (1999) in press.

12. Zelenin, A. K.; Trudell, M. L.; and Gilardi, R. D., J. Heterocyclic Chem., **35**, *151* (1998).

13. Zelenin, A. K.; Stevens, E. D.; and Trudell, M. L., Struct. Chem., **8**, *373* (1997).

CHAPTER 3

THERMAL DECOMPOSITION STUDIES OF FURAZAN COMPOUNDS

3.1 Structure-Property Relations

The crystal structures of seven of the compounds in Table 1.1 will be compared in Chapter 4. Some of the physical properties in Table 2.1 and behavior upon pyrolysis can be related to these structures. Because each H atom is bonded to N, the number of hydrogen bonding possibilities in these compounds roughly increases with the number of hydrogen atoms in the formula. Hydrogen bonding of course adds cohesion to the crystal lattice and therefore the number of hydrogen atoms might roughly correlate with the melting points and tendency to evaporate. As can be seen in Table 2.1, the average melting points of compounds with the same number of H atoms (given parenthetically here) generally follow this trend, i.e. 248°C (4 H), 140°C (2 H), 81°C (0 H). The exception is DAHzF, which has 6 H atoms, but a melting point of 192°C. As will be discussed below however, this compound loses H_2 from the –N(H)N(H)- linkage at the melting point. Hence the H atom count in relation to the melting characteristics is deceptive and this compound might better be included in the category with 4 H atoms rather than 6 H atoms.

During pyrolysis studies it was observed in some cases that evaporation of the intact parent molecule occurred before the rapid decomposition stage was reached. In fact only the azoxy-bridged compounds with one or two NH_2 groups (ANAF and DAAF) did not exhibit some evaporation. Consistent with this observation is the fact that nearest neighbor N-H ····N(ring) and N-H ····O(azoxy) attractive interactions both result in short distances (2.33-2.41 Å and 2.52 Å, respectively) in the solid state. These close contacts enable the azoxy oxygen atom also to interact intermolecularly with a ring N atom of opposite partial charge. Such significant cohesive forces may also be responsible for the fact that the density of ANAF and DAAF is the highest of the compounds studied in this work (1.856 g/cm^3 and 1.840 g/cm^3, respectively).

3.2 Decomposition of Furazans

The decomposition temperatures for the furazan compounds listed in Table 2.1 measured by DSC in a closed Al pan lie in the 160-255 °C range with most lying near 200 °C. The temperature of decomposition does not appear to correlate in any easily recognized way with the structure or formula of the parent compound. The temperature of the strongly exothermic decomposition stage is well separated from the melting point in most of the compounds. Exceptions are DAHzF, DAAzF and DAAF. In these cases multiple phases are probably present during fast decomposition in the T-jump/FTIR spectroscopy experiment, however, as is discussed below, the initial step of DAHzF decomposition is unusual and involves the reaction of the hydrazo bridge in which the ring remains in tact. When flash pyrolyzed at temperatures above 300-450°C and

pressures above 5 atm Ar, all of the compounds except DAF and DAHzF instantly release only readily identified gaseous products. DAF and DAHzF have additional absorptions at 2100-2200 cm^{-1} that overlap the peaks of HNCO and CO and are the result of other products. DAF was previously shown to liberate ammonium dicyanamide $NH_4[N(CN)_2]$ which absorbs in this range.[1] Table 3.1 summarizes the mole fractions of the gaseous products that can be identified clearly. The atom balance was completed for all compounds except DAF and DAHzF by assuming the necessary amount of IR inactive N_2 and H_2. T-Jump/Raman spectroscopy measurements were conducted on DNAF to quantify N_2. The mole fraction of N_2 observed in this measurement (0.49) compares very well with that required for completion of the elemental atom balance on the basis of the

Table 3.1 Mole fractions of decomposition products

		Flash Pyrolysis Products						
compound	formula	CO_2	CO	HCN	O	NH_3	N_2	H_2
DAF	$C_2N_4H_4O$	0.024	0.213	0.626	0.034	0.104		
ANF	$C_2N_4H_2O_3$	0.111	0.252	0.027	0.001		0.377	0.232
DNF	$C_2N_4O_5$							
DAAzF	$C_4N_8H_4O_2$	0.023	0.199	0.436	0.025		0.316	
ANAzF	$C_4N_8H_2O_4$							
DNAzF	$C_4N_8O_6$	0.227	0.277				0.496	
DAAF	$C_4N_8H_4O_3$	0.011	0.321	0.203	0.006		0.36	0.099
ANAF	$C_4N_8H_2O_5$	0.086	0.376	0.018			0.429	0.092
DNAF	$C_4N_8O_7$	0.31	0.201				0.489	
DAHzF	$C_4N_8H_6O_2$	0.027	0.012	0.548	0.048	0.078	0.201	
ANHzF	$C_4N_8H_4O_4$							
DNHzF	$C_4N_8H_2O_6$	0.275	0.142				0.45	0.109

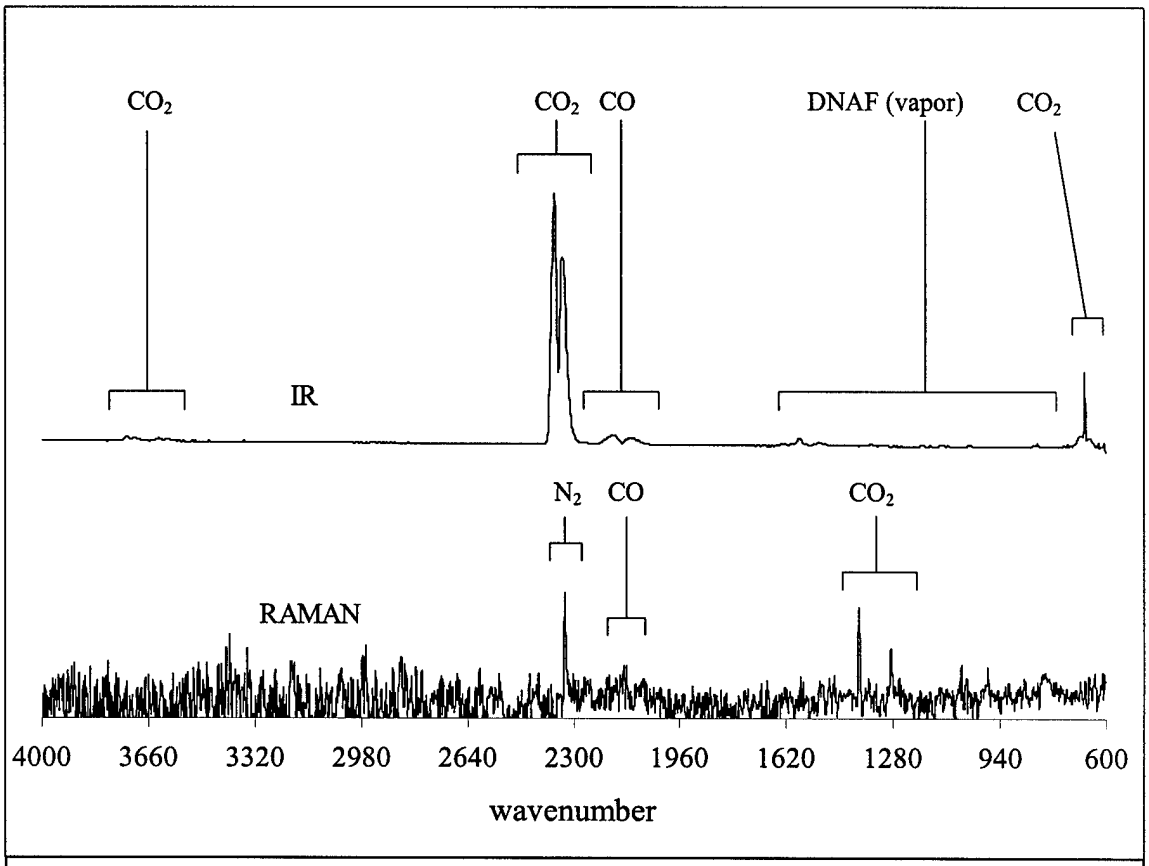

Figure 3.1 T-Jump/FTIR (350°C, 12 atmospheres argon) and T-Jump/Raman (350°C, 9 atmospheres argon) of DNAF

other products and the DNAF formula (0.49). Representative spectra of these experiments are given in Figure 3.1. The elemental atom balance of DNAF ($C_4N_8O_7$) based on the mole fractions of the gaseous products is $C_{4.16}N_{7.7}O_{6.7}$ when normalized to each element and averaged. Except in the two compounds where other unquantified products are present, the atom balances for all compounds are within 5% for each element.

The nitrogen oxides like NO, N_2O and NO_2 are notably absent from the products when the compounds are flash heated. NO and N_2O were hypothesized to be non-

equilibrium products of combustion of the nitro and azoxy derivatives of these compounds.[2] We obtained no evidence of any nitrogen oxides at any conditions of flash pyrolysis, although NO_2 and N_2O have been observed as products of slow pyrolysis.[3]

Only a few trends stand out in the gaseous products as a function of the parent structure. A plot of the CO/CO_2 ratio vs. the O/C ratio in the parent compound is shown in Figure 3.2. This plot does not include DAAF or DAAzF, which do not fit the trend. As noted above DAAF decomposes without melting and this phase difference may upset the comparison. In the case of DAAzF other unquantified products interfere with the quantification of CO making it difficult to know the CO/CO_2 ratio. However, the general pattern of increasing CO_2 content with increasing O/C ratio holds for all of the compounds except for DAAF and DAAzF. The correlation in Figure 3.2 indicates that the oxidation of C by O is efficient in most of these compounds.

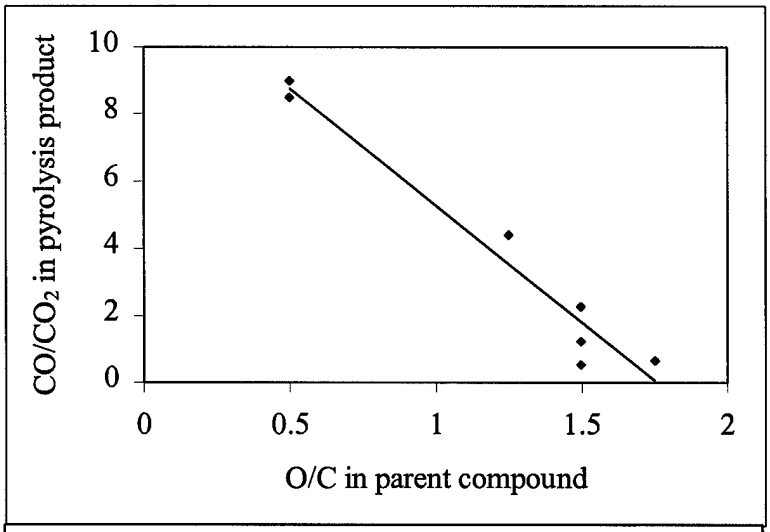

Figure 3.2 Comparison of CO/CO_2 ratio in the pyrolysis products and oxygen / carbon ratio in parent molecule.

HNCO is observed as a pyrolysis product when $H \geq C$ in the stoichiometry of the parent compound. This is generally the case for all of the diamines. The H atoms are

divided among the HNCO and HCN products, and the pattern that H must be greater than C indicates that H preferentially favors forming HCN before HNCO during the decomposition process.

HCN is a major product when the compound possesses two NH_2 groups, but is a minor product when one NH_2 or any NH groups are present. The behavior of the NH groups is understandable because the -N(H)N(H)- hydrazo linkage initially decomposes to form the –N=N- azo group and H_2. This process is evident in the residues collected after heating DAHzF and DNHzF in a DSC pan to 10 °C above the melting point. It is also apparent from the T-jump/FTIR spectroscopy experiment on DAHzF shown in Fig. 3.3 where the vaporized compound that appears before the violently exothermic

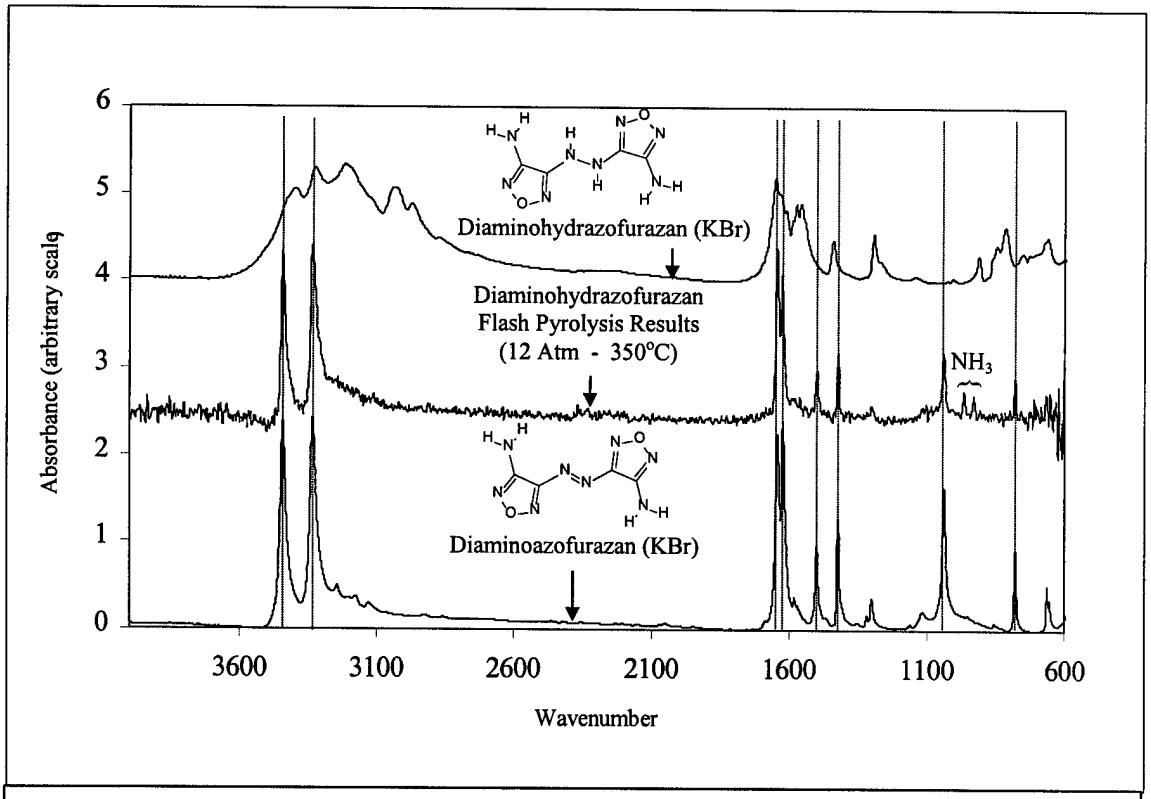

Figure 3.3 Infrared spectra showing the conversion of DAHzF to DAAzF

decomposition stage has undergone reaction E3.1. The same result was obtained for DNHzF in accordance with reaction E3.2. Therefore the initial reaction of the hydrazo-bridged compounds is E3.1 and E3.2 after melting occurs.

$$DAHzF \longrightarrow DAAzF + H_2 \qquad (E3.1)$$

$$DNHzF \longrightarrow DNAzF + H_2 \qquad (E3.2)$$

On the basis of E3.1 and E3.2, it is reasonable to predict that the burning rates within the pairs DAHzF-DAAzF and DNHzF-DNAzF would be similar since H_2 is lost before the energetic backbone decomposes. Beyond this observation, burning rate predictions based on the pyrolysis products observed for these compounds appear to be ambiguous. For example, DNAzF burns slightly faster than DNAF[2] despite the fact that the more exothermic product CO_2 dominates CO in DNAF, whereas the reverse is the case for DNAzF. On the other hand DNAF burns about ten times faster than DAAF[2] in accordance with the much more exothermically formed set of products from DNAF shown in Table 3.1.

3.3 References

37. Stoner, C. E. Jr. and Brill, T. B., Combust. Flame, **83**, *302*, (1991).

38. Sinditskii, V. P.; Dong, H. W.; Serushkin, V.; Fogelzang, A. E.; and Sheremetev, A. B., Int. Ann. Conf. ICT, 29th (Energetic Materials), *170-1*, (1998).

39. Löbbecke, S.; Pfeil, A.; and Krause, H., Int. Ann. Conf. ICT, 29th, (1998).

Chapter 4

X-RAY CRYSTALLOGRAPHY OF FURAZAN COMPOUNDS

4.1 Introduction

DAF and ANF have been subjected to structural determination.[1] The crystal structures of two of the two-ring furazans, DNAzF[2] and ANAF,[3] have been published previously. Crystals of the other five of the seven two-ring compounds that were studied in this thesis were obtained and studied by x-ray crystallography.

The bonding in the furazan ring is formally aromatic and its structure is expected to be planar. This is true for all of the structures now available. Therefore, the bridging linkage of the two rings and the structural details of the substituents are the unique features of these structures. Theoretically the two ring compounds with conjugated linkages could have eight geometric isomers within their planar orientations. Four of these result from a cis configuration about the interior linkage and the other four result from a trans configuration. These are shown in Figure 4.1. If the substituent on a given ring is brought towards the double bond, the ring is referred to as proximal (P) to the interior linkage. If the substituent is turned away from the interior linkage, the ring is referred to as distal (D). Combinations of P and D isomerism on the two rings form the four possible orientations mentioned above. The trans configuration seems to be favored for steric reasons and is found in all of the compounds studied here.

cis (P, P) cis (P, D) cis (D, P) cis (D, D)

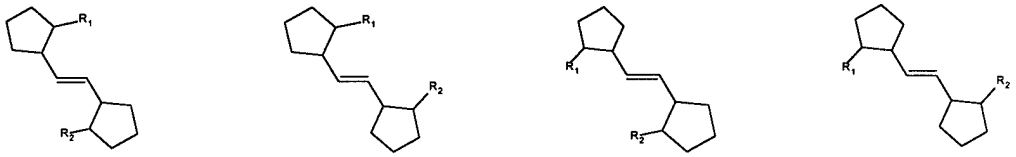

trans (P, P) trans (P, D) trans (D, P) trans (D, D)

Figure 4.1 Geometric isomers of two-ring furazans

All seven structures will be compared here. The structure of each compound will be discussed briefly along with the bond distances and angles. The chapter concludes with an analysis of the general trends.

4.2 Structure of DAAzF

Both of the substituents are amine groups in this molecule. The ring system has the trans (P, P) isomerization and the ring dimensions are practically identical giving the molecule a C_2 axis. Interestingly, the molecules stack directly above one another in the crystal lattice. Seen side on, this appears to be a series of stacked plates similar to the planar stacks in graphite. The structure is shown in Figure 4.2 and the crystallographic data are given in Tables 4.1 – 4.3.

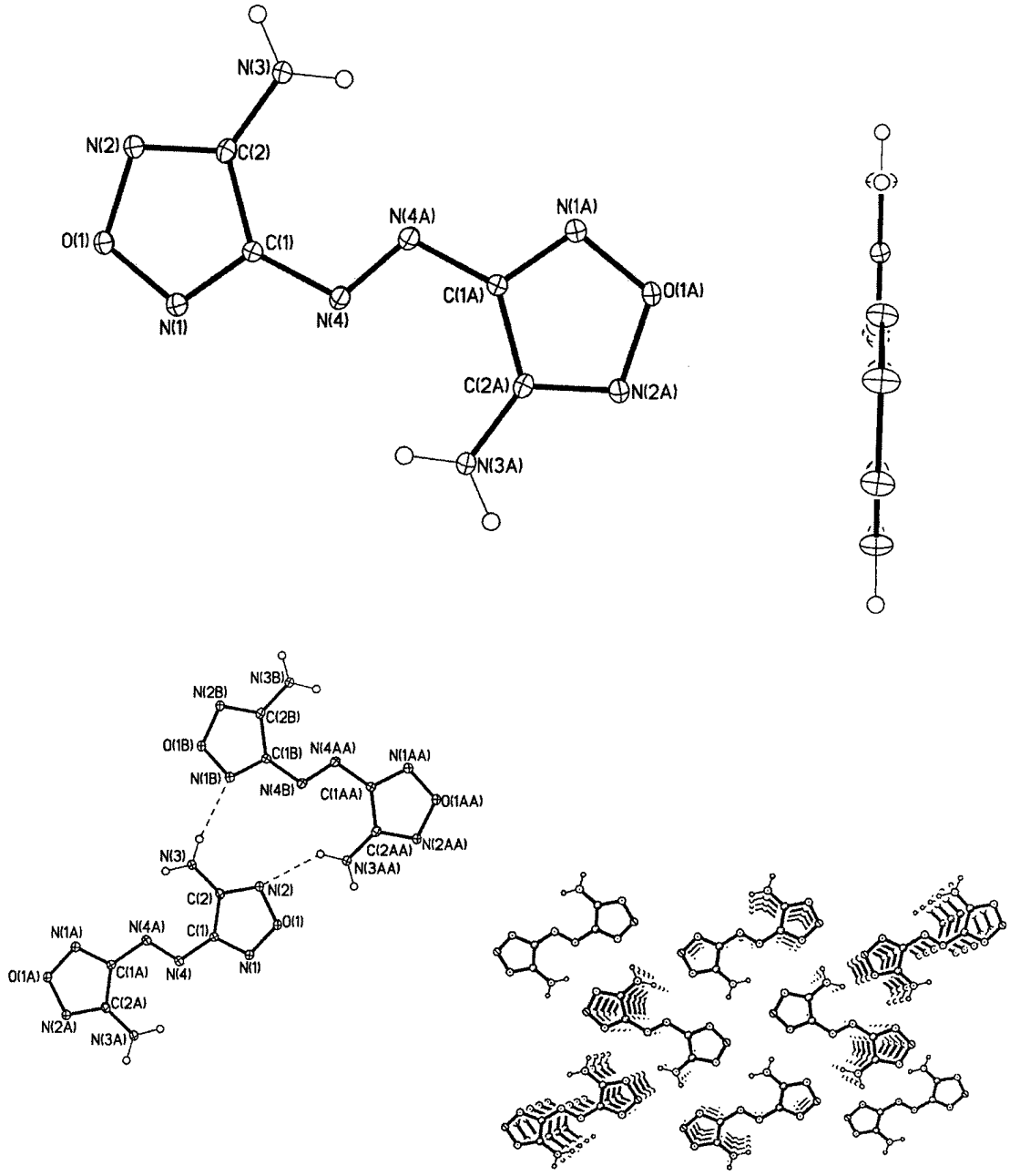

Figure 4.2 Crystallographically derived images of DAAzF. Clockwise from top left: Single molecule (top view), single molecule (end view), packing diagram, and intermolecular positioning

Table 4.1 Crystal data and structure refinement for DAAzF.

Empirical formula	$C_4H_4N_8O_2$	
Formula weight	196.13	
Temperature	173(2) K	
Wavelength	0.71073 Å	
Crystal system	Monoclinic	
Space group	$P2_{1/c}$	
Unit cell dimensions	a = 3.7431(10) Å	α= 90°.
	b = 10.053(3) Å	β= 95.957(5)°.
	c = 9.848(3) Å	γ = 90°.
Volume	368.58(17) $Å^3$	
Z	2	
Density (calculated)	1.767 Mg/m^3	
Absorption coefficient	0.801 mm^{-1}	
F(000)	1064	
Crystal size	0.48 x 0.20 x 0.14 mm^3	
Theta range for data collection	2.90 to 28.28°.	
Index ranges	$-4 \leqslant h \leqslant 4$, $-12 \leqslant k \leqslant 11$, $-12 \leqslant l \leqslant 11$	
Reflections collected	1630	
Independent reflections	770 [R(int) = 0.0245]	
Completeness to theta = 28.28°	84.8 %	
Absorption correction	Empirical from SADABS	
Max. and min. transmission	0.8962 and 0.6999	
Refinement method	Full-matrix least-squares on F^2	
Data / restraints / parameters	770 / 0 / 64	
Goodness-of-fit on F^2	0.856	
Final R indices [I>2sigma(I)]	R1 = 0.0514, wR2 = 0.1418	
R indices (all data)	R1 = 0.0582, wR2 = 0.1494	
Largest diff. peak and hole	0.428 and -0.257 $e.Å^{-3}$	

Table 4.2 Atomic coordinates (x 10^4) and equivalent isotropic displacement parameters ($Å^2$ x 10^3) for DAAzF. U(eq) is defined as one third of the trace of the orthogonalized U_{ij} tensor.

	x	y	z	U(eq)
O(1)	4035(5)	3743(2)	4168(2)	24(1)
N(4)	5656(5)	524(2)	5282(2)	18(1)
C(1)	4447(6)	1666(2)	4563(2)	16(1)
N(1)	5531(5)	2826(2)	5062(2)	22(1)
C(2)	2165(6)	1854(2)	3304(2)	17(1)
N(2)	1946(5)	3145(2)	3065(2)	22(1)
N(3)	484(5)	940(2)	2495(2)	23(1)

Table 4.3 Bond lengths [Å] and angles [°] for DAAzF.

O(1)-N(1)	1.355(2)	N(1)-O(1)-N(2)	111.72(14)
O(1)-N(2)	1.406(2)	N(4)#1-N(4)-C(1)	111.7(2)
N(4)-N(4)#1	1.266(3)	N(1)-C(1)-N(4)	117.9(2)
N(4)-C(1)	1.399(3)	N(1)-C(1)-C(2)	109.77(17)
C(1)-N(1)	1.313(3)	N(4)-C(1)-C(2)	132.37(19)
C(1)-C(2)	1.443(3)	C(1)-N(1)-O(1)	105.64(18)
C(2)-N(2)	1.319(3)	N(2)-C(2)-N(3)	123.7(2)
C(2)-N(3)	1.331(3)	N(2)-C(2)-C(1)	107.60(19)
		N(3)-C(2)-C(1)	128.66(18)
		C(2)-N(2)-O(1)	105.27(18)

Symmetry transformations used to generate equivalent atoms:
#1 -x+1,-y,-z+1

4.3 Structure of DNAzF

The structure and crystallographic data for DNAzF can be found in the literature.[2] Both of the substituents are nitro groups in this molecule. The ring system has the trans (P, D) isomerization, which brings both nitro groups to the same side of the molecule. The nitro group on the proximal position is orthogonal to the plane of the rest of the molecule. This is likely to minimize steric interactions between the electron-rich oxygen atoms of the nitro groups. Therefore despite the potential to have many symmetry elements, the molecule has only the identity. In the crystal lattice, the plane of one molecule lies essentially orthogonal to the neighboring molecule. The orthogonal oriented nitro groups are arranged adjacent to each other. This set of alternating perpendicular molecules results in an approximate parallelogram shaped cage of four molecules when viewed from the side.

The nitro group which lies in the molecular plane has a slightly shorter C-N bond distance than that in the adjacent ring. Also the O-N bond distances of the NO_2 group are slightly shorter. This pattern suggests that the π system of the nitro group and the π system of the ring are conjugated to some extent. The structure is shown in Figure 4.3.

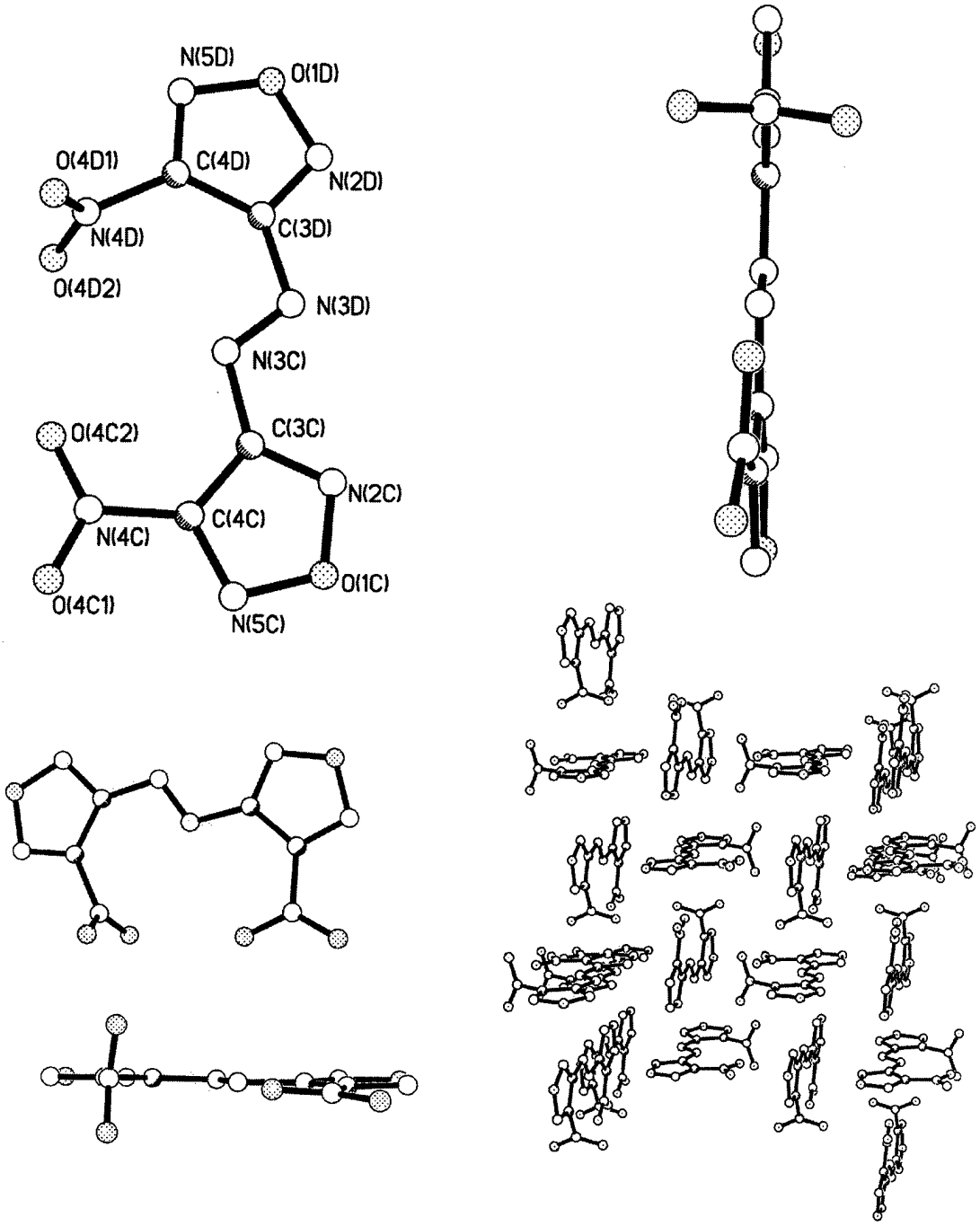

Figure 4.3 Crystallographically derived images of DNAzF. Clockwise from top left: Single molecule (top view), single molecule (end view), packing diagram, and intermolecular positioning

4.4 Structure of DAAF

Both of the substituents are amino groups in this molecule. The ring system has the trans (D, D) isomerization. However, the oxygen on one of the nitrogen atoms in the azoxy linkage breaks the molecular symmetry. The presence of the oxygen atom also causes lengthening of the C-N(azoxy) bond. Furthermore, interior ring angle centered on the carbon atom bonded to the azoxy group has a larger angle and the interior ring angle centered on the other carbon has a smaller angle than the other ring. All of these distortions can be attributed to the electron withdrawing capacity of the oxygen atom of the azoxy linkage. It should also be noted that the molecule packs in the crystal lattice with the azoxy oxygen in 50/50 disorder. As such, its interactions are an average of both orientations.

In the crystal lattice, the molecules are positioned end to side. This orientation probably results from intermolecular hydrogen bonding between the nitrogen in the 5-position of one ring and hydrogen atoms on the amino group of a neighboring molecule. While the amino group of the first molecule can interact with the azoxy oxygen atom and the nitrogen in the 2- position of the neighboring molecule. The structure is shown in Figure 4.4 and the crystallographic data are given in Tables 4.4 – 4.6.

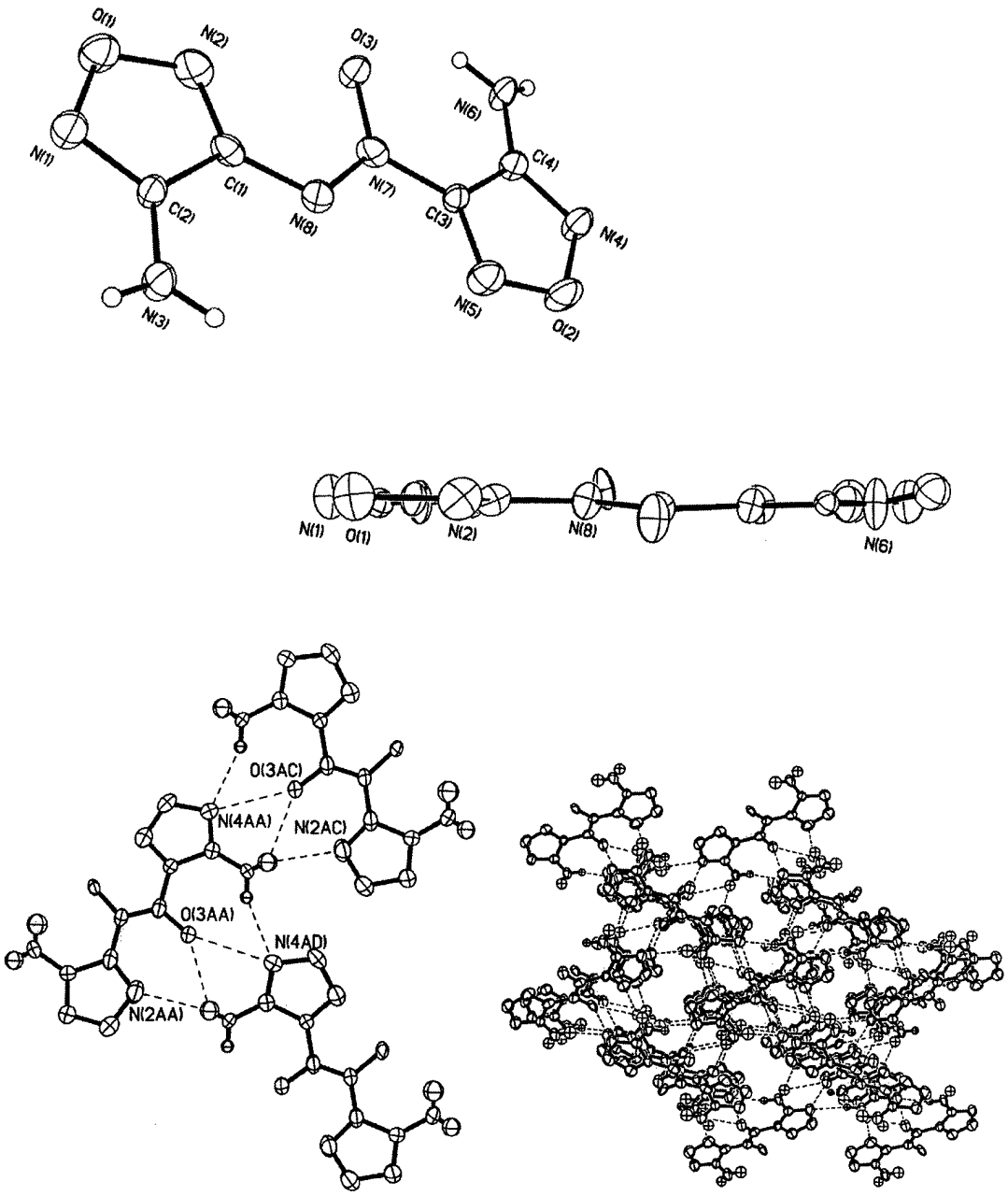

Figure 4.4 Crystallographically derived images of DAAF. Clockwise from top left: Single molecule (top view), single molecule (end view), packing diagram, and intermolecular positioning

Table 4.4 Crystal data and structure refinement for DAAF.

Empirical formula	$C_4H_4N_8O_3$	
Formula weight	212.15	
Temperature	233(2) K	
Wavelength	0.71073 Å	
Crystal system	Monoclinic	
Space group	$P2_{1/c}$	
Unit cell dimensions	a = 9.3212(8) Å	α= 90°.
	b = 9.6326(9) Å	β= 91.3434(19)°.
	c = 8.9004(8) Å	γ = 90°.
Volume	798.9(2) $Å^3$	
Z	4	
Density (calculated)	1.764 Mg/m^3	
Absorption coefficient	0.152 mm^{-1}	
F(000)	432	
Crystal size	0.30 x 0.30 x 0.20 mm^3	
Theta range for data collection	2.19 to 25.50°.	
Index ranges	$-11 \leqslant h \leqslant 10$, $-9 \leqslant k \leqslant 11$, $-9 \leqslant l \leqslant 10$	
Reflections collected	3157	
Independent reflections	1422 [R(int) = 0.0481]	
Completeness to theta = 25.50°	95.3 %	
Absorption correction	Empirical	
Max. and min. transmission	0.9703 and 0.9559	
Refinement method	Full-matrix least-squares on F^2	
Data / restraints / parameters	1422 / 0 / 161	
Goodness-of-fit on F^2	1.834	
Final R indices [I>2sigma(I)]	R1 = 0.0825, wR2 = 0.2428	
R indices (all data)	R1 = 0.1069, wR2 = 0.2607	
Largest diff. peak and hole	0.331 and -0.296 $e.Å^{-3}$	

Table 4.5 Atomic coordinates (x 10^4) and equivalent isotropic displacement parameters ($Å^2$ x 10^3) for DAAF. U(eq) is defined as one third of the trace of the orthogonalized U_{ij} tensor.

	x	y	z	U(eq)
O(1)	7765(4)	5970(3)	1043(4)	49(1)
O(2)	7355(4)	13501(3)	-907(4)	49(1)
N(1)	8869(4)	6291(4)	2090(4)	43(1)
N(2)	7265(4)	7134(5)	328(4)	46(1)
N(3)	9961(5)	8379(5)	2850(5)	42(1)
N(4)	6249(4)	13286(4)	-1978(4)	42(1)
N(5)	7734(4)	12299(4)	-195(4)	44(1)
N(6)	4987(4)	11299(4)	-2779(5)	38(1)
N(7)	6961(4)	9940(4)	-379(4)	33(1)
N(8)	7953(4)	9580(4)	536(4)	33(1)
C(1)	8031(4)	8171(5)	900(5)	33(1)
C(2)	9034(4)	7645(4)	2005(5)	30(1)
C(3)	6912(4)	11369(4)	-804(4)	29(1)
C(4)	5963(4)	11956(4)	-1921(5)	33(1)
O(3)	6016(4)	9115(4)	-976(4)	39(1)
O(3')	8937(15)	10549(15)	1040(15)	36(3)

Table 4.6 Bond lengths [Å] and angles [°] for DAAF.

O(1)-N(2)	1.366(5)	N(2)-O(1)-N(1)	111.4(3)
O(1)-N(1)	1.406(5)	N(5)-O(2)-N(4)	111.6(3)
O(2)-N(5)	1.362(5)	C(2)-N(1)-O(1)	105.4(3)
O(2)-N(4)	1.403(5)	C(1)-N(2)-O(1)	105.4(4)
N(1)-C(2)	1.316(5)	C(4)-N(4)-O(2)	105.4(4)
N(2)-C(1)	1.323(6)	C(3)-N(5)-O(2)	104.5(4)
N(3)-C(2)	1.334(6)		
N(4)-C(4)	1.309(6)	N(8)-N(7)-O(3)	125.2(4)
N(5)-C(3)	1.290(6)	N(8)-N(7)-C(3)	116.9(3)
N(6)-C(4)	1.334(6)	O(3)-N(7)-C(3)	117.9(3)
N(7)-N(8)	1.267(5)	N(7)-N(8)-O(3')	119.7(7)
N(7)-O(3)	1.291(5)	N(7)-N(8)-C(1)	116.7(3)
N(7)-C(3)	1.428(5)	O(3')-N(8)-C(1)	123.5(7)
N(8)-O(3')	1.377(14)	N(2)-C(1)-N(8)	128.3(4)
N(8)-C(1)	1.397(6)	N(2)-C(1)-C(2)	109.6(4)
C(1)-C(2)	1.433(6)	N(8)-C(1)-C(2)	122.2(4)
C(3)-C(4)	1.432(5)	N(1)-C(2)-N(3)	124.6(4)
		N(1)-C(2)-C(1)	108.3(4)
		N(3)-C(2)-C(1)	127.1(4)
		N(5)-C(3)-N(7)	122.9(4)
		N(5)-C(3)-C(4)	111.6(4)
		N(7)-C(3)-C(4)	125.4(4)
		N(4)-C(4)-N(6)	125.4(4)
		N(4)-C(4)-C(3)	106.9(4)
		N(6)-C(4)-C(3)	127.7(4)

4.5 Structure of ANAF

The structure and crystallographic data can be found in the literature.[3] Special note should be made that this lattice contains ethanol and water of solvation. As such, an extensive and complicated system of hydrogen bonding arises. Several unsuccessful attempts were made to grow crystals without these solvents. Although ethanol could be excluded, water could not. The structure provided is the best structure available at this time.

The molecule adopts the trans (D, P) isomer. The ring with the nitro group is oriented D and the ring with the amino group is oriented P in this molecule. This brings both substituents to the same side of the molecule but forces the azoxy oxygen to the other side. Furthermore, it allows an oxygen atom of the nitro group to hydrogen bond with a hydrogen atom on the amino group.

The N-O bond distance of 1.24 Å in the linkage is shorter than its analog in DAAF (1.29 Å). The extensive interactions of the azoxy oxygen atom in DAAF with neighboring hydrogen atoms probably lengthens this bond. Although the azoxy oxygen atom in ANAF does interact with a neighboring molecule, the interactions are with the nitrogen atoms of the azoxy group rather than hydrogen atoms. However, some intermolecular hydrogen bonding does occur. The outermost hydrogen atom of the amino group interacts with the outermost nitrogen atom of the aminated ring of the neighbor molecule. The same interaction is reciprocated by the ring nitrogen and a hydrogen atom of the neighboring amino group. The structure is shown in Figure 4.5.

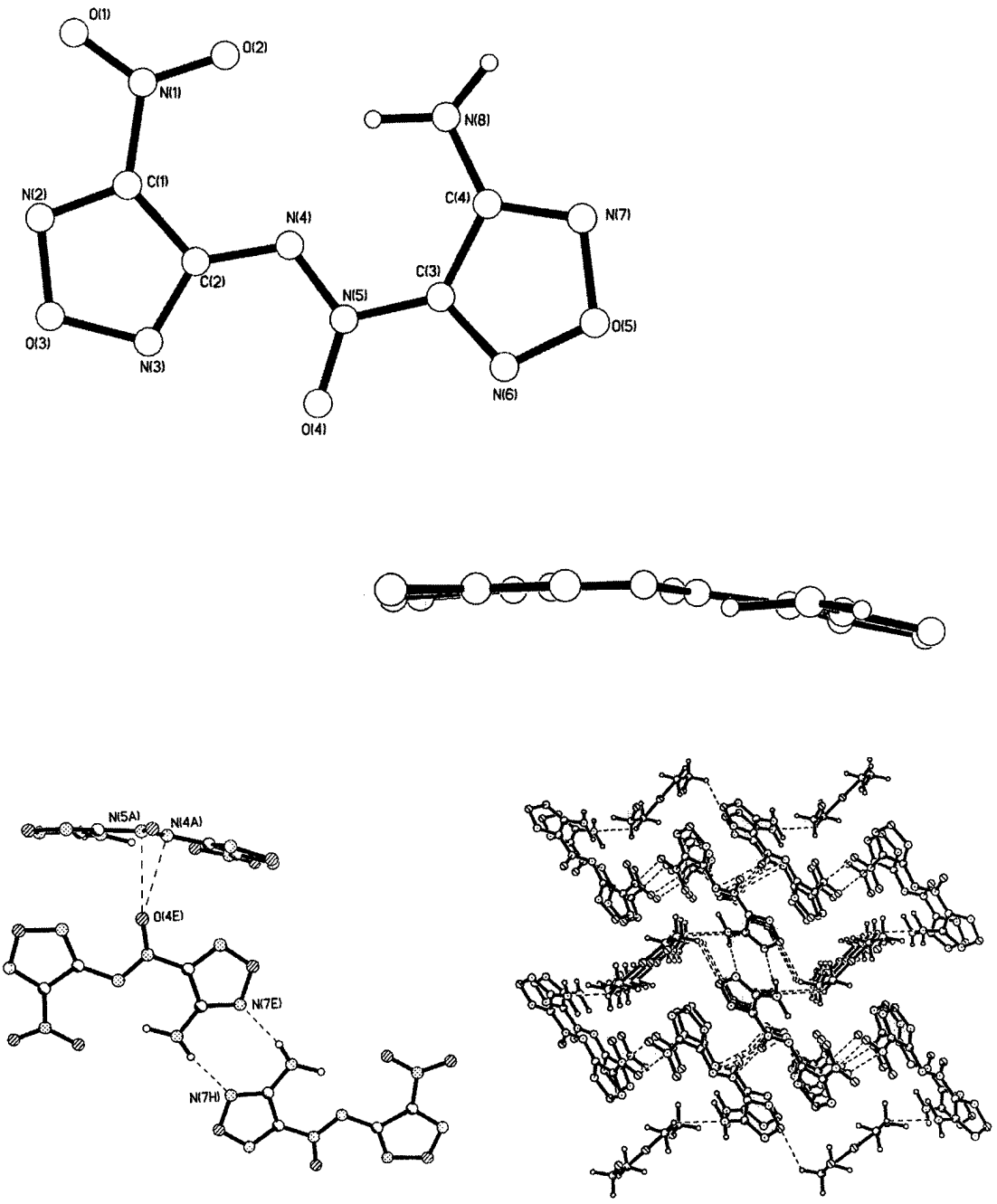

Figure 4.5 Crystallographically derived images of ANAF. Clockwise from top left: Single molecule (top view), single molecule (end view), packing diagram, and intermolecular positioning

4.6 Structure of DNAF

Both substituents are nitro groups in this molecule. The ring system is the trans (P, D) isomer which brings both nitro groups to the same side of the molecule and forces the oxygen of the azoxy linkage to the other side. Like DNAzF, one of the nitro groups is perpendicular to the plane of the molecule. The N-O bonds in this nitro group are about 0.015 Å longer and the bond angle is about 2 degrees greater than those in the other nitro group. Unlike DNAzF however, there is little significant difference between the bond lengths to the nitro groups and the rings remain very similar to each other.

The N-O bond in the azoxy linkage is the shortest of the three azoxy molecules (1.23 Å vs. 1.24 Å and 1.29 Å). As in the previous cases, the N-C bond involving the azoxy is longer by about 0.05 Å than the azo N-C bond.

Similarly to DNAzF, the molecule packs orthogonally. Similarly to ANAF, the azoxy oxygen interacts with the nitrogen atoms in the neighboring azoxy group. Unlike DNAzF however, the placement of the twisted nitro group alternates from one molecule to the next. Nevertheless the packing of the crystal lattices of DNAF and DNAzF are very similar. The structure is shown in Figure 4.6 and the crystallographic data are given in Tables 4.7 – 4.9.

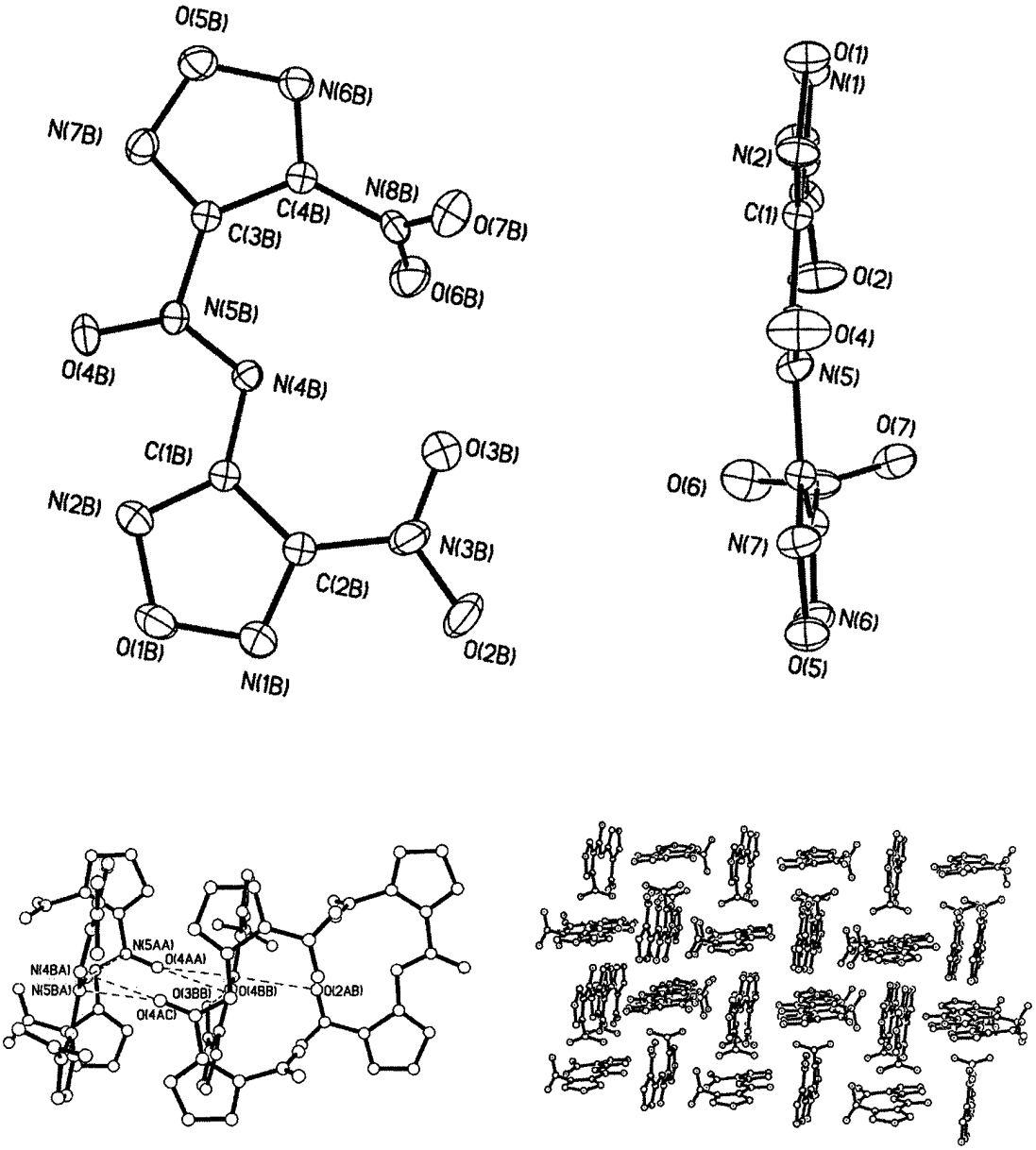

Figure 4.6 Crystallographically derived images of DNAF. Clockwise from top left: Single molecule (top view), single molecule (end view), packing diagram, and intermolecular positioning

Table 4.7 Crystal data and structure refinement for DNAF.

Empirical formula	$C_4N_8O_7$	
Formula weight	272.12	
Temperature	173(2) K	
Wavelength	0.71073 Å	
Crystal system	Triclinic	
Space group	$P\bar{1}$	
Unit cell dimensions	a = 10.5298(2) Å	α= 83.1000(10)°.
	b = 10.54980(10) Å	β= 65.9230(10)°.
	c = 10.5957(2) Å	γ = 66.26°.
Volume	982.31(3) $Å^3$	
Z	4	
Density (calculated)	1.840 Mg/m^3	
Absorption coefficient	0.175 mm^{-1}	
F(000)	544	
Crystal size	0.40 x 0.30 x 0.20 mm^3	
Theta range for data collection	2.30 to 28.26°.	
Index ranges	$-2 \leqslant h \leqslant 13$, $-7 \leqslant k \leqslant 8$, $-4 \leqslant l \leqslant 13$	
Reflections collected	4276	
Independent reflections	1817 [R(int) = 0.0351]	
Completeness to theta = 28.26°	37.4 %	
Absorption correction	None	
Max. and min. transmission	0.9658 and 0.9332	
Refinement method	Full-matrix least-squares on F^2	
Data / restraints / parameters	1817 / 0 / 303	
Goodness-of-fit on F^2	1.634	
Final R indices [I>2sigma(I)]	R1 = 0.0548, wR2 = 0.1755	
R indices (all data)	R1 = 0.0612, wR2 = 0.1861	
Largest diff. peak and hole	0.462 and -0.276 $e.Å^{-3}$	

Table 4.8 Atomic coordinates (x 10^4) and equivalent isotropic displacement parameters ($Å^2$ x 10^3) for DNAF. U(eq) is defined as one third of the trace of the orthogonalized U_{ij} tensor.

	x	y	z	U(eq)
C(1)	-1059(5)	3086(5)	3211(6)	28(1)
C(1B)	1939(4)	6783(5)	2392(5)	29(1)
C(2)	-1977(4)	3304(4)	2436(5)	28(1)
C(2B)	2790(4)	7519(5)	2396(5)	31(1)
C(3)	2765(4)	2384(5)	2564(5)	28(1)
C(3B)	-1866(4)	7393(5)	3089(5)	29(1)
C(4)	3576(5)	2309(5)	1153(5)	33(1)
C(4B)	-2712(4)	8836(5)	3241(5)	31(1)
N(1)	-3381(4)	3693(4)	3277(4)	38(1)
N(1B)	4181(4)	6684(5)	2140(5)	44(2)
N(2)	-1925(4)	3318(4)	4511(4)	36(1)
N(2B)	2809(4)	5455(4)	2161(4)	39(1)
N(3)	-1534(4)	3167(4)	968(4)	34(1)
N(3B)	2324(4)	8980(5)	2668(5)	48(2)
N(4)	528(3)	2680(4)	2537(4)	26(1)
N(4B)	403(3)	7423(4)	2633(4)	28(1)
N(5)	1173(4)	2651(4)	3358(4)	32(1)
N(5B)	-263(4)	6629(5)	2732(4)	29(2)
N(6)	4974(4)	2062(4)	873(4)	45(2)
N(6B)	-4130(4)	9069(5)	3626(4)	41(2)
N(7)	3620(4)	2246(4)	3223(4)	38(2)
N(7B)	-2751(4)	6722(4)	3368(4)	39(1)
N(8)	3085(4)	2416(6)	-4(5)	44(2)
N(8B)	-2217(5)	9968(5)	3030(6)	39(2)
O(1)	-3374(3)	3706(4)	4559(3)	42(1)
O(1B)	4208(3)	5415(4)	1995(4)	51(1)
O(2)	-243(4)	3039(4)	213(4)	65(2)
O(2B)	3284(4)	9430(4)	2414(5)	65(2)
O(3)	-2472(3)	3173(4)	576(3)	51(1)
O(3B)	989(4)	9650(5)	3184(6)	97(2)
O(4)	637(4)	2872(4)	4613(4)	57(1)
O(4B)	233(4)	5361(4)	2633(4)	51(1)
O(5)	5003(3)	2035(3)	2184(3)	41(1)
O(5B)	-4175(3)	7769(4)	3716(4)	47(1)
O(6)	3266(4)	1347(5)	-491(4)	67(2)
O(6B)	-1586(4)	10217(4)	1839(6)	58(2)
O(7)	2532(4)	3592(4)	-323(4)	54(1)
O(7B)	-2468(4)	10558(5)	4083(5)	66(2)

Table 4.9 Bond lengths [Å] and angles [°] for DNAF.

C(1)-N(2)	1.290(6)	N(2)-C(1)-N(4)	130.1(3)
C(1)-N(4)	1.418(6)	N(2)-C(1)-C(2)	108.7(4)
C(1)-C(2)	1.444(4)	N(4)-C(1)-C(2)	121.2(5)
C(1B)-N(2B)	1.315(6)	N(2B)-C(1B)-N(4B)	128.0(4)
C(1B)-N(4B)	1.401(4)	N(2B)-C(1B)-C(2B)	108.9(3)
C(1B)-C(2B)	1.404(6)	N(4B)-C(1B)-C(2B)	123.0(4)
C(2)-N(1)	1.293(6)	N(1)-C(2)-N(3)	121.0(3)
C(2)-N(3)	1.437(6)	N(1)-C(2)-C(1)	109.5(4)
C(2B)-N(1B)	1.300(5)	N(3)-C(2)-C(1)	129.5(4)
C(2B)-N(3B)	1.442(6)	N(1B)-C(2B)-C(1B)	110.7(5)
C(3)-N(7)	1.304(4)	N(1B)-C(2B)-N(3B)	119.6(4)
C(3)-C(4)	1.379(6)	C(1B)-C(2B)-N(3B)	129.7(3)
C(3)-N(5)	1.457(6)	N(7)-C(3)-C(4)	110.4(4)
C(3B)-N(7B)	1.309(5)	N(7)-C(3)-N(5)	119.0(4)
C(3B)-C(4B)	1.410(6)	C(4)-C(3)-N(5)	130.5(3)
C(3B)-N(5B)	1.448(4)	N(7B)-C(3B)-C(4B)	110.5(3)
C(4)-N(6)	1.294(5)	N(7B)-C(3B)-N(5B)	119.8(4)
C(4)-N(8)	1.490(5)	C(4B)-C(3B)-N(5B)	129.7(4)
C(4B)-N(6B)	1.299(5)	N(6)-C(4)-C(3)	110.8(3)
C(4B)-N(8B)	1.446(6)	N(6)-C(4)-N(8)	119.3(5)
N(1)-O(1)	1.364(5)	C(3)-C(4)-N(8)	129.8(3)
N(1B)-O(1B)	1.353(5)	N(6B)-C(4B)-C(3B)	109.2(4)
N(2)-O(1)	1.392(3)	N(6B)-C(4B)-N(8B)	121.0(4)
N(2B)-O(1B)	1.394(4)	C(3B)-C(4B)-N(8B)	129.9(3)
N(3)-O(3)	1.215(3)	C(2)-N(1)-O(1)	104.8(3)
N(3)-O(2)	1.223(5)	C(2B)-N(1B)-O(1B)	104.1(4)
N(3B)-O(3B)	1.200(5)	C(1)-N(2)-O(1)	104.6(3)
N(3B)-O(2B)	1.206(5)	C(1B)-N(2B)-O(1B)	103.3(4)
N(4)-N(5)	1.295(4)	O(3)-N(3)-O(2)	125.1(4)
N(4B)-N(5B)	1.264(5)	O(3)-N(3)-C(2)	117.1(4)
N(5)-O(4)	1.224(5)	O(2)-N(3)-C(2)	117.7(3)
N(5B)-O(4B)	1.225(5)	O(3B)-N(3B)-O(2B)	124.8(5)
N(6)-O(5)	1.398(5)	O(3B)-N(3B)-C(2B)	116.6(4)
N(6B)-O(5B)	1.382(5)	O(2B)-N(3B)-C(2B)	118.5(4)
N(7)-O(5)	1.368(5)	N(5)-N(4)-C(1)	113.8(4)
N(7B)-O(5B)	1.385(5)	N(5B)-N(4B)-C(1B)	116.6(4)
N(8)-O(6)	1.210(5)	O(4)-N(5)-N(4)	130.3(4)
N(8)-O(7)	1.213(6)	O(4)-N(5)-C(3)	119.4(3)
N(8B)-O(6B)	1.217(5)	N(4)-N(5)-C(3)	110.2(4)
N(8B)-O(7B)	1.223(6)	O(4B)-N(5B)-N(4B)	129.8(3)
		O(4B)-N(5B)-C(3B)	118.2(4)
		N(4B)-N(5B)-C(3B)	111.9(4)
		C(4)-N(6)-O(5)	103.0(4)
		C(4B)-N(6B)-O(5B)	104.9(4)
		C(3)-N(7)-O(5)	103.6(4)
		C(3B)-N(7B)-O(5B)	103.5(4)
		O(6)-N(8)-O(7)	128.4(4)
		O(6)-N(8)-C(4)	117.2(4)
		O(7)-N(8)-C(4)	114.4(5)
		O(6B)-N(8B)-O(7B)	127.3(6)
		O(6B)-N(8B)-C(4B)	117.0(5)
		O(7B)-N(8B)-C(4B)	115.7(6)
		N(1)-O(1)-N(2)	112.4(3)
		N(1B)-O(1B)-N(2B)	112.9(3)
		N(7)-O(5)-N(6)	112.1(2)
		N(6B)-O(5B)-N(7B)	112.0(3)

4.7 Structure of DAHzF

Both substituents are amino groups in this molecule. The bridging linkage in this molecule is not constrained with respect to rotation. As a result, this molecule is not planar. However, the individual rings and the amino groups on them are coplanar. Also the hydrogen atoms in the hydrazo linkage are coplanar with the adjacent ring. However, the two ring planes are nearly orthogonal. The geometries of the rings are nearly identical. This might give the molecule a C_2 axis but the symmetry is broken by a water of crystallization. Hydrogen bonding between the outermost nitrogen atom of one ring and the water molecule breaks the symmetry. The other hydrogen atom of H_2O interacts with an interior ring nitrogen of a neighboring molecule. The result is the effacing of two molecules with respect to the planes of one of each of their ring systems. The other ring systems therefore become essentially coplanar. This forms a closely packed pair, which repeats in the crystal lattice. The structure is shown in Figure 4.7 and the crystallographic data are given in Tables 4.10 – 4.12.

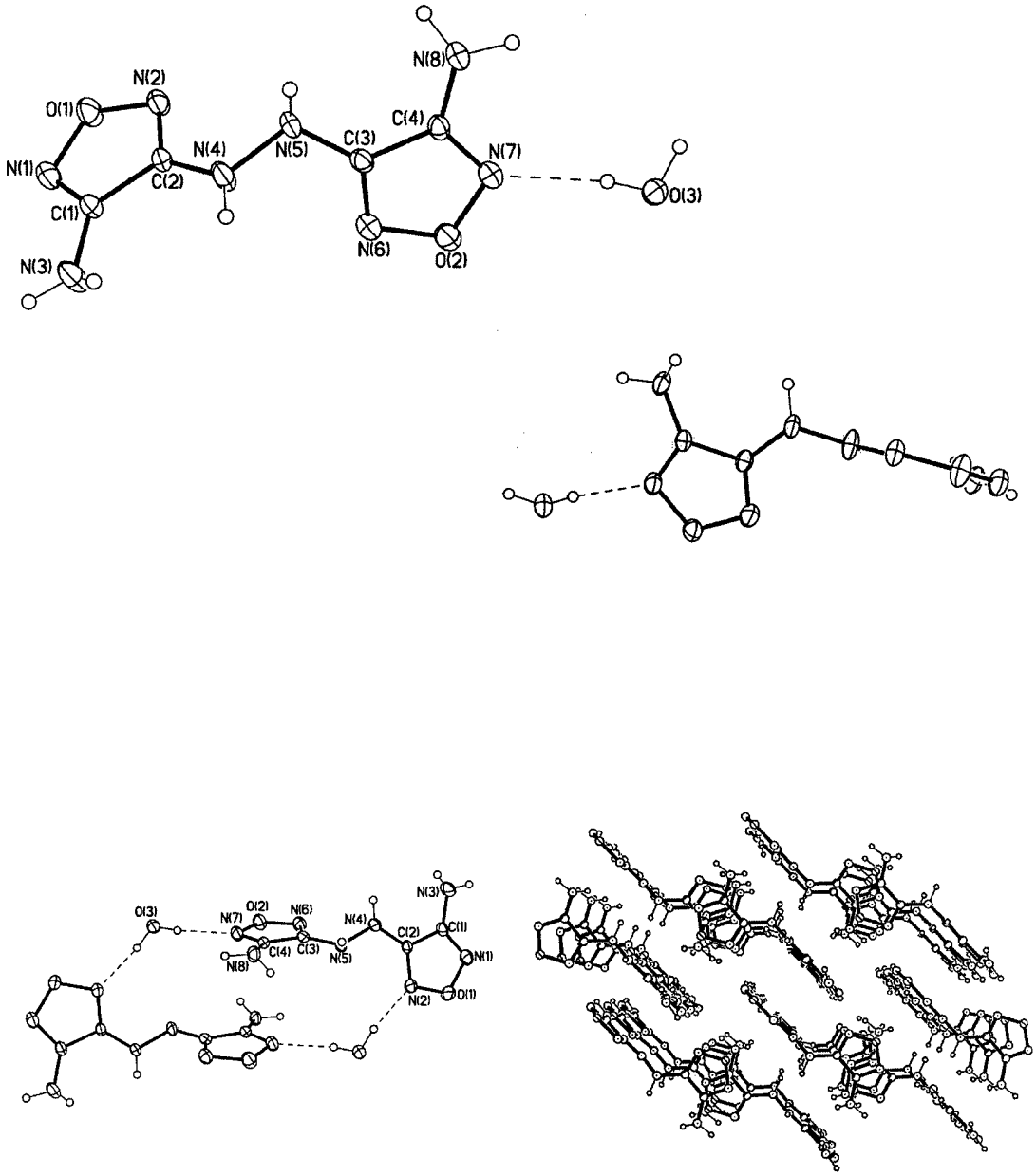

Figure 4.7 Crystallographically derived images of DAHzF. Clockwise from top left: Single molecule (top view), single molecule (end view), packing diagram, and intermolecular positioning

Table 4.10 Crystal data and structure refinement for DAHzF.

Empirical formula	$C_4H_8N_8O_3$	
Formula weight	216.18	
Temperature	248(2) K	
Wavelength	0.71073 Å	
Crystal system	Triclinic	
Space group	$P\bar{1}$	
Unit cell dimensions	a = 6.9071(16) Å	α= 82.29(2)°.
	b = 7.5490(18) Å	β= 84.83(3)°.
	c = 8.564(2) Å	γ = 84.79(2)°.
Volume	439.32(19) $Å^3$	
Z	2	
Density (calculated)	1.634 Mg/m^3	
Absorption coefficient	0.139 mm^{-1}	
F(000)	224	
Crystal size	0.30 x 0.20 x 0.20 mm^3	
Theta range for data collection	2.41 to 22.48°.	
Index ranges	$-1 \leqslant h \leqslant 7$, $-8 \leqslant k \leqslant 8$, $-9 \leqslant l \leqslant 9$	
Reflections collected	1433	
Independent reflections	1093 [R(int) = 0.0288]	
Completeness to theta = 22.48°	94.7 %	
Absorption correction	None	
Max. and min. transmission	0.9727 and 0.9595	
Refinement method	Full-matrix least-squares on F^2	
Data / restraints / parameters	1093 / 0 / 169	
Goodness-of-fit on F^2	1.137	
Final R indices [I>2sigma(I)]	R1 = 0.0351, wR2 = 0.0936	
R indices (all data)	R1 = 0.0432, wR2 = 0.1039	
Extinction coefficient	0.047(10)	
Largest diff. peak and hole	0.163 and -0.190 $e.Å^{-3}$	

Table 4.11 Atomic coordinates (x 10^4) and equivalent isotropic displacement parameters ($Å^2$ x 10^3) for DAHzF. U(eq) is defined as one third of the trace of the orthogonalized U_{ij} tensor.

	x	y	z	U(eq)
O(1)	4991(2)	17416(2)	5246(2)	47(1)
O(2)	1907(2)	9341(2)	8580(2)	42(1)
O(3)	2270(3)	5577(2)	11670(2)	39(1)
N(1)	3238(3)	18042(3)	4580(2)	43(1)
N(2)	4627(3)	16128(2)	6561(2)	36(1)
N(3)	-47(4)	17342(3)	5170(3)	47(1)
N(4)	1763(4)	14866(3)	7728(2)	43(1)
N(5)	2729(3)	13766(2)	8910(2)	34(1)
N(6)	1935(3)	11145(2)	7923(2)	39(1)
N(7)	2442(3)	9135(2)	10138(2)	37(1)
N(8)	3183(3)	11116(3)	11859(2)	37(1)
C(1)	1889(3)	17180(3)	5428(3)	31(1)
C(2)	2757(3)	15970(3)	6652(2)	27(1)
C(3)	2459(3)	11969(3)	9044(3)	30(1)
C(4)	2761(3)	10722(3)	10433(3)	28(1)

Table 4.12 Bond lengths [Å] and angles [°] for DAHzF.

O(1)-N(1)	1.401(3)	N(1)-O(1)-N(2)	109.75(16)
O(1)-N(2)	1.406(2)	N(7)-O(2)-N(6)	109.94(16)
O(2)-N(7)	1.402(2)	C(1)-N(1)-O(1)	106.03(17)
O(2)-N(6)	1.402(2)	C(2)-N(2)-O(1)	105.33(17)
N(1)-C(1)	1.296(3)	C(2)-N(4)-N(5)	120.3(2)
N(2)-C(2)	1.302(3)	C(3)-N(5)-N(4)	116.0(2)
N(3)-C(1)	1.367(3)	C(3)-N(6)-O(2)	104.94(17)
N(4)-C(2)	1.342(3)	C(4)-N(7)-O(2)	106.36(17)
N(4)-N(5)	1.399(3)	N(1)-C(1)-N(3)	125.8(2)
N(5)-C(3)	1.374(3)	N(1)-C(1)-C(2)	109.2(2)
N(6)-C(3)	1.305(3)	N(3)-C(1)-C(2)	124.9(2)
N(7)-C(4)	1.299(3)	N(2)-C(2)-N(4)	126.0(2)
N(8)-C(4)	1.358(3)	N(2)-C(2)-C(1)	109.7(2)
C(1)-C(2)	1.431(3)	N(4)-C(2)-C(1)	124.3(2)
C(3)-C(4)	1.432(3)	N(6)-C(3)-N(5)	125.2(2)
		N(6)-C(3)-C(4)	110.26(19)
		N(5)-C(3)-C(4)	124.5(2)
		N(7)-C(4)-N(8)	124.7(2)
		N(7)-C(4)-C(3)	108.5(2)
		N(8)-C(4)-C(3)	126.7(2)

4.8 Structure of DNHzF

Both substituents are nitro groups in this molecule. Like DAHzF, there is no conjugation through the bridging linkage to force the two ring systems into the same plane. Also like DAHzF the rings and their respective nitro groups as well as the adjacent hydrazo hydrogen each form a plane and those planes are nearly orthogonal to each other.

There is no solvent in the lattice and interactions different from DAHzF dominate the structure. There is hydrogen bonding between the nitro oxygen atoms on one molecule and one of the hydrogen atoms in the hydrazo linkage of another. The other hydrogen atom hydrogen bonds to the nitro oxygen of yet a third molecule. Additionally, an interaction exists between the outermost ring nitrogen and the nitrogen of a neighboring nitro group. This is most likely the result of interactions between the somewhat polarized π system of the ring and the electron-rich nitro group. The structure is shown in Figure 4.8 and the crystallographic data are given in Tables 4.13 – 4.15.

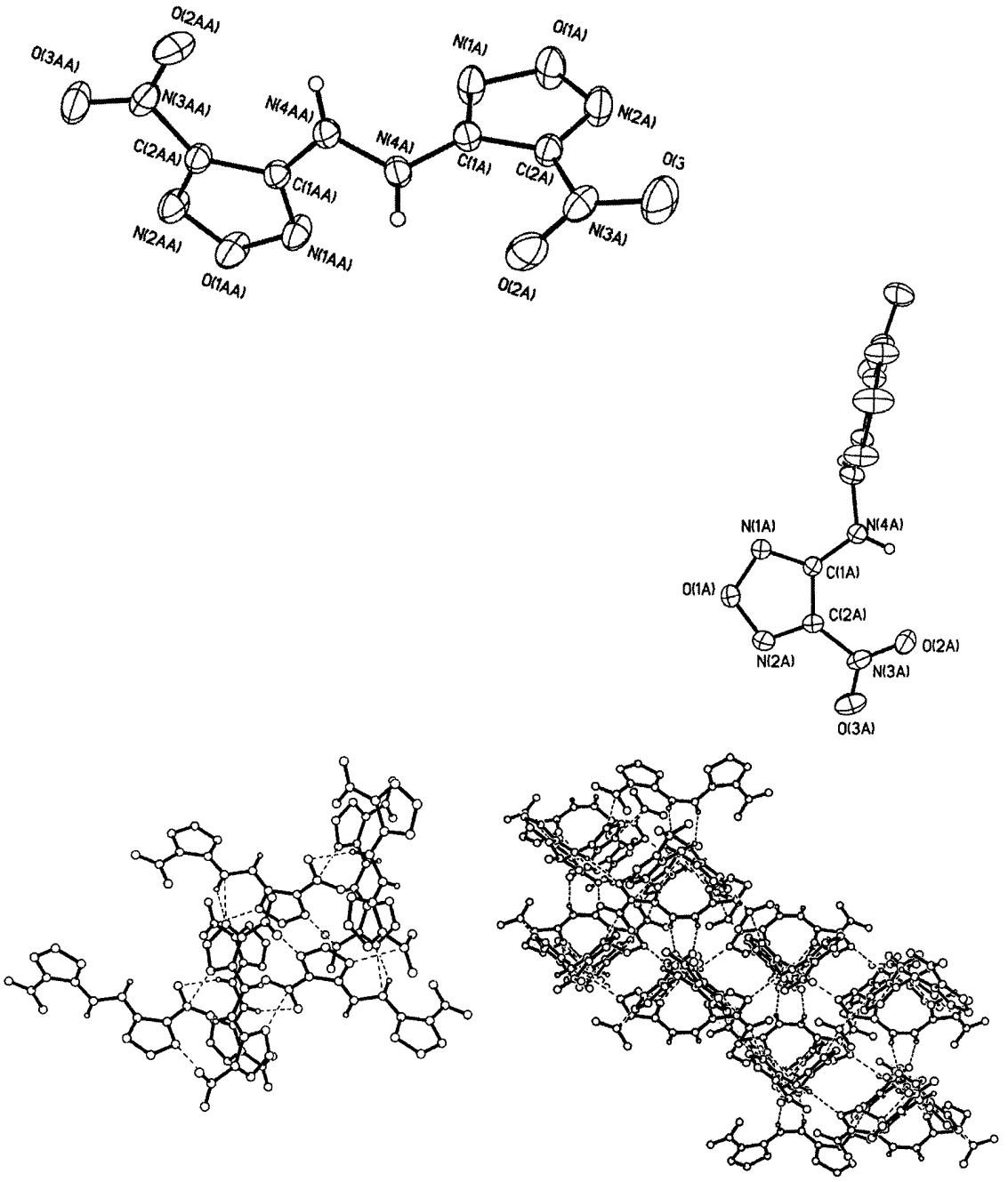

Figure 4.8 Crystallographically derived images of DNHzF. Clockwise from top left: Single molecule (top view), single molecule (end view), packing diagram, and intermolecular positioning

Table 4.13 Crystal data and structure refinement for DNHzF

Empirical formula	$C_4H_2N_8O_6$	
Formula weight	258.14	
Temperature	213(2) K	
Wavelength	0.71073 Å	
Crystal system	Orthorhombic	
Space group	Pccn	
Unit cell dimensions	a = 12.1292(3) Å	α= 90°.
	b = 12.4461(2) Å	β= 90°.
	c = 12.6773(2) Å	γ = 90°.
Volume	1913.77(5) $Å^3$	
Z	8	
Density (calculated)	1.792 Mg/m^3	
Absorption coefficient	0.167 mm^{-1}	
F(000)	1040	
Crystal size	0.35 x 0.35 x 0.35 mm^3	
Theta range for data collection	2.34 to 25.99°.	
Index ranges	$-13 \leqslant h \leqslant 11$, $-15 \leqslant k \leqslant 15$, $-15 \leqslant l \leqslant 15$	
Reflections collected	7270	
Independent reflections	1756 [R(int) = 0.0407]	
Completeness to theta = 25.99°	93.2 %	
Absorption correction	Empirical	
Max. and min. transmission	0.9439 and 0.9439	
Refinement method	Full-matrix least-squares on F^2	
Data / restraints / parameters	1756 / 0 / 163	
Goodness-of-fit on F^2	1.326	
Final R indices [I>2sigma(I)]	R1 = 0.0780, wR2 = 0.1676	
R indices (all data)	R1 = 0.0968, wR2 = 0.1787	
Largest diff. peak and hole	0.284 and -0.244 $e.Å^{-3}$	

Table 4.14 Atomic coordinates (x 10^4) and equivalent isotropic displacement parameters ($Å^2$ x 10^3) for DNHzF. U(eq) is defined as one third of the trace of the orthogonalized U_{ij} tensor.

	x	y	z	U(eq)
O(1B)	5350(3)	1324(3)	4141(3)	62(1)
O(1A)	5476(3)	-739(3)	-1543(3)	74(1)
O(2B)	3591(3)	3734(3)	2888(3)	68(1)
O(2A)	7966(3)	149(3)	757(2)	64(1)
O(3B)	5008(3)	3893(2)	1843(2)	56(1)
O(3A)	6798(3)	1415(3)	384(3)	79(1)
N(1B)	6366(3)	1484(3)	3635(3)	51(1)
N(1A)	6082(3)	-1656(3)	-1276(3)	59(1)
N(2B)	4580(3)	2037(3)	3812(3)	54(1)
N(2A)	5824(4)	140(3)	-1011(3)	62(1)
N(3B)	4509(3)	3485(3)	2582(3)	47(1)
N(3A)	7170(4)	514(3)	285(3)	52(1)
N(4B)	6982(3)	2736(3)	2388(3)	49(1)
N(4A)	7578(3)	-1948(2)	-143(3)	45(1)
C(1B)	6189(3)	2290(3)	2999(3)	38(1)
C(1A)	6800(3)	-1322(3)	-593(3)	39(1)
C(2B)	5080(3)	2630(3)	3125(3)	40(1)
C(2A)	6631(4)	-206(3)	-440(3)	43(1)

Table 4.15 Bond lengths [Å] and angles [°] for DNHzF.

O(1B)-N(2B)	1.355(5)	N(2B)-O(1B)-N(1B)	111.8(3)
O(1B)-N(1B)	1.403(5)	N(2A)-O(1A)-N(1A)	112.0(3)
O(1A)-N(2A)	1.352(5)	C(1B)-N(1B)-O(1B)	104.4(3)
O(1A)-N(1A)	1.399(5)	C(1A)-N(1A)-O(1A)	104.6(3)
O(2B)-N(3B)	1.219(5)	C(2B)-N(2B)-O(1B)	105.0(3)
O(2A)-N(3A)	1.224(5)	C(2A)-N(2A)-O(1A)	104.3(3)
O(3B)-N(3B)	1.226(4)	O(2B)-N(3B)-O(3B)	126.1(4)
O(3A)-N(3A)	1.215(5)	O(2B)-N(3B)-C(2B)	118.3(4)
N(1B)-C(1B)	1.305(5)	O(3B)-N(3B)-C(2B)	115.6(4)
N(1A)-C(1A)	1.296(5)	O(3A)-N(3A)-O(2A)	125.8(4)
N(2B)-C(2B)	1.293(5)	O(3A)-N(3A)-C(2A)	118.1(4)
N(2A)-C(2A)	1.292(5)	O(2A)-N(3A)-C(2A)	116.1(4)
N(3B)-C(2B)	1.444(5)	C(1B)-N(4B)-N(4B)#1	118.0(4)
N(3A)-C(2A)	1.440(5)	C(1A)-N(4A)-N(4A)#2	118.4(4)
N(4B)-C(1B)	1.355(5)	N(1B)-C(1B)-N(4B)	123.5(4)
N(4B)-N(4B)#1	1.387(7)	N(1B)-C(1B)-C(2B)	108.4(4)
N(4A)-C(1A)	1.350(5)	N(4B)-C(1B)-C(2B)	128.0(4)
N(4A)-N(4A)#2	1.387(6)	N(1A)-C(1A)-N(4A)	124.5(4)
C(1B)-C(2B)	1.419(6)	N(1A)-C(1A)-C(2A)	108.0(4)
C(1A)-C(2A)	1.418(5)	N(4A)-C(1A)-C(2A)	127.5(4)
		N(2B)-C(2B)-C(1B)	110.5(4)
		N(2B)-C(2B)-N(3B)	121.1(4)
		C(1B)-C(2B)-N(3B)	128.4(4)
		N(2A)-C(2A)-C(1A)	111.0(4)
		N(2A)-C(2A)-N(3A)	119.7(4)
		C(1A)-C(2A)-N(3A)	129.1(4)

Symmetry transformations used to generate equivalent atoms:
#1 -x+3/2,-y+1/2,z #2 -x+3/2,-y-1/2,z

4.9 Summary

One of the earliest attractions to this class of compounds for the application of energetic materials was the fact that the furazan ring is aromatic and should be planar. Furthermore, conjugated systems of the rings should also be coplanar. With the exceptions of one nitro group on DNAzF and DNAF, and the bridging linkage in DAHzF and DNHzF, that has proven to be the case for these molecules. Even in the case of the hydrazo linkages, the individual ring systems are planar and have a tendency to stack in the crystal lattice with rings facing rings of neighboring molecules. Also, as anticipated, this results in reasonably high densities. A noteworthy exception to this pattern of coplanarity occurs when both substituents are nitro groups. Initially this was attributed to steric factors within the molecule, but a trans (D, D) isomerization as observed in DAAF would tend to be favored if steric factors dominate. It seems instead, that intermolecular interactions are primarily responsible for the variety of ring position isomerizations observed. No cis conformations about the bridging linkages were found and probably are excluded by intramolecular steric effects. Although rings substituted with nitro groups tended to have slightly more distortion than those with amino groups, no major deviations from compound to compound were observed.

4.10 References

1. Batsanov, A. S. and Struchkov, Y. T., Zh. Strukt. Khim., **26**, *65-1*, (1985)

2. Zelenin, A. K.; Trudell, M. L.; and Gilardi, R. D., J. Heterocyclic Chem., **35**, *151* (1998).

3. Zelenin, A. K.; Stevens, E. D.; and Trudell, M. L., Struct. Chem., **8**, *373* (1997).

CHAPTER 5

DENSITY FUNCTIONAL THEORETICAL INVESTIGATION OF FURAZAN COMPOUNDS

5.1 Heats of Formation

The measured standard heats of formation for several of the target compounds have been reported by two groups.[1,2] One group reported primarily on the compounds containing primarily amino functionality,[1] while the other group reported on the compounds containing primarily nitro functionality.[2] While isolated thermochemical data for these compounds can be found in other references,[3-6] most refer back to the references in Table 2.1. Where other data are provided, the numbers agree very poorly with those previously cited. Hence it is difficult then to trust the numbers given. As thermochemical data for energetic materials are used extensively within the energetic materials community, an attempt was made to rectify the discrepancies found in the literature.

The approach selected was a quantum mechanical computational evaluation of each of the target compounds. The density functional theory method (DFT) was selected due to the fact that its accuracy in electron correlation of Hartree Fock energy rivals that of significantly more computationally expensive methods, such as second and third order Møller-Plesset perturbation methods and quadratic configuration interaction methods.

The Gaussian 98[7] package was used to optimize the geometry of each compound using the B3LYP[8,9] method and the 6-31G* basis set (B3LYP/6-31G*). The geometry optimization was necessary to obtain an energy at a state which most closely models the ground state of the compound. It also establishes the geometry for which the vibrational analysis will be performed. Next a vibrational analysis was performed at the same computational level on each compound. The vibrational analysis provides vibrational as well as rotational corrections to the ground state energy. Next, the same DFT analysis was performed on CH_4, H_2O, N_2, and H_2. As standard heats of formation are known for these compounds, heats of formation for each of the furazan compounds could be calculated by Hess's Law relating the heats and calculated energies through the theoretical decomposition reaction (E5.1) of each compound into the aforementioned small molecules. Equation (E5.2) shows the relationship between the calculated energies and heats of formation used to calculate heats of formation for the furazan molecules. Very little if any H_2 is formed by most of the furazan compounds. Therefore, the coefficient for H_2 is negative. This is chemically and thermodynamically equivalent to adding the required hydrogen to the left side of the reaction. Table 5.1 provides the

$$C_X N_Y O_Z H_A \rightarrow xCH_4 + \tfrac{Y}{2} N_2 + zH_2O + (\tfrac{A}{2} - 2x - z)H_2 \qquad \text{(E5.1)}$$

$$\Delta H^o_{f\,furazan} = E_{furazan} - [x(E_{CH_4} + \Delta H^o_{f\,CH_4}) + \tfrac{Y}{2}(E_{N_2} + \Delta H^o_{f\,N_2}) + z(E_{H_2O} + \Delta H^o_{f\,H_2O}) + (\tfrac{A}{2} - 2x - z)(E_{H_2} + \Delta H^o_{f\,H_2})] \qquad \text{(E5.2)}$$

Table 5.1 Values used to calculate Heats of Formation

Compound	E* (hartrees)	$\Delta H_{f\,calc}$ (Kcal/mol)
DAF	-372.67	29.09
ANF	-521.82	-1.34
DNF	-670.94	-14.13
DAAzF	-742.93	114.03
ANAzF	-892.06	95.61
DNAzF	-1041.18	77.51
DAAF	-818.11	84.58
ANAF	-967.24	62.47
DNAF	-1116.35	52.38
DAHzF	-744.13	93.97
ANHzF	-893.27	65.11
DNHzF	-1042.41	36.64
		$\Delta H_{f\,actual}$ (Kcal/mol)
CH_4	-40.47	-17.90
N_2	-109.52	0.00
H_20	-76.38	-57.80
H_2	-1.16	0.00

* Energies are corrected for zero point vibrational and rotational energy

standard heats of formation used for the small molecules and the absolute energies (in Hartrees) for all compounds calculated.

The geometry optimization algorithm is based on a single molecule with no intermolecular interactions at absolute zero. The vibrational analysis, however, takes into account the more relevant conditions of one atmosphere pressure and 273 K. As a result, the model is most appropriate to the molecule in the gas phase, which is not the standard state for any of the furazan compounds. Also, some error is introduced by the difference in the nature of the bonds between the parent compounds and the decomposition product compounds. For instance, all of the carbon in the parent compounds is classically sp^2 hybridized while the carbon in methane is sp^3 hybridized. Nevertheless, most of the error associated with this breakdown of assumptions is systematic such that the differences between one furazan molecule and another should be fairly reliable although the absolute ΔH_f^o may not be reliable. That is, trends are valid and permit predictions of the thermochemical data for

compounds on which no experiments have been run. Furthermore, the trends might clarify the contradictory numbers reported for any particular compound.

Once the thermochemical data were calculated, however it became very apparent that the trends could not be associated in the way hoped. The reason for this is that the calculated trends were remarkably different from those reported before, although the reported data are too sparse for any detailed trend analysis. The calculated heats of formation are provided in Table 5.1 and shown graphically in Figure 5.1. From the previously reported numbers, the substitution of an amino group with a nitro group results in an increase in the heat of formation. This is based on a comparison of DAF vs. ANF, DAAzF vs. DNAzF, and DAAF vs. DNAF. However, the heats of formation

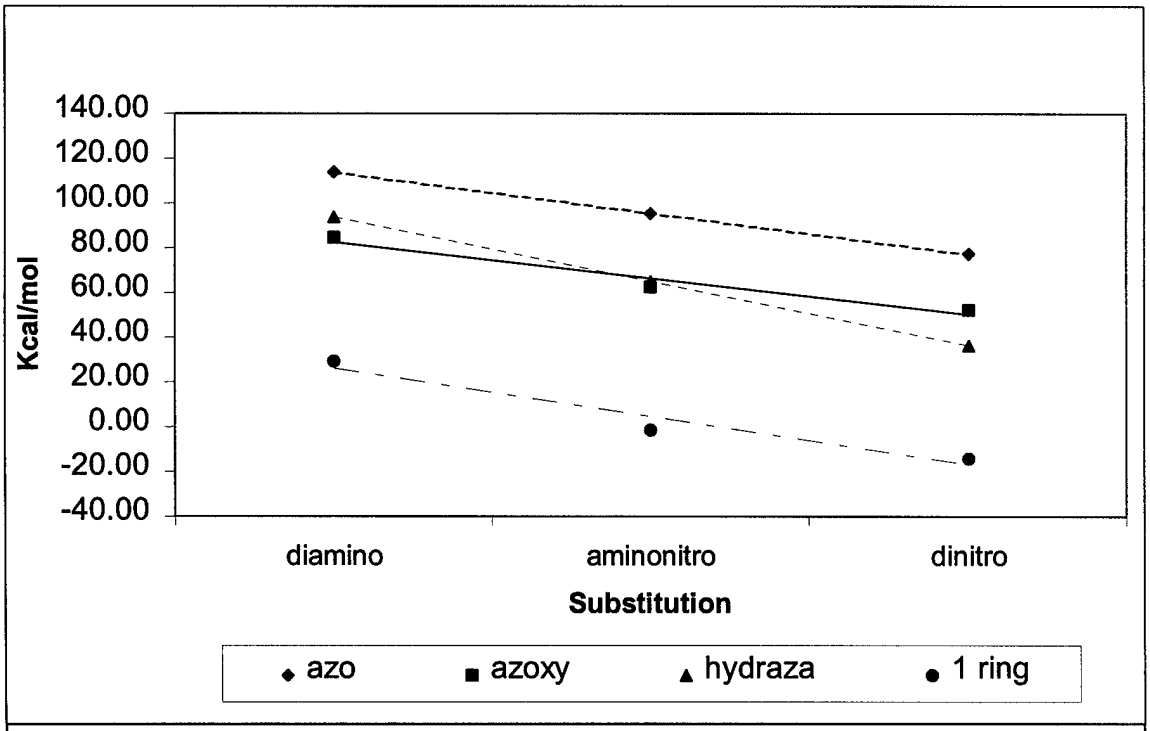

Figure 5.1 Calculated heats of formation for furazan compounds

Table 5.2 Comparison of heats of amino and nitro groups

Compounds for comparison	ΔH_f (Kcal/mol)	$\Delta\Delta H_f$ (Kcal/mol)
methylamine	-11.32 [10]	
nitromethane	-27.03 [11]	-15.71
ethylamine	-20.22 [12]	
nitroethane	-34.45 [11]	-14.23
1-propanamine	-24.28 [13]	
1-nitropropane	-39.95 [11]	-15.67
2-propanamine	-26.87 [13]	
2-nitropropane	-43.14 [10]	-16.27
1,3-diaminobenzene	-1.89 [14]	
1,3-aminonitrobenzene	-8.18 [15]	-6.29

calculated here show the opposite trend. In support of the current work are the data in Table 5.2. Substitution of $-NH_2$ by $-NO_2$ in more common molecules for which the thermochemical data are well established supports the trend found here on the reduction in the heat of formation. Hence the calculated trend for the furazans seems reasonable. In fact, the change in heat of formation associated with the substitution found in the calculated data is very similar to the trend found in Table 5.2. Although this calculated trend raises questions about the reported data, unfortunately it does not resolve every issue. The uncertainty within the assumptions and the error in the calculations themselves renders the absolute values of the heats of formation dubious, although the differences are reasonable. Any thermochemical analysis based on ΔH_f values currently available should be considered questionable.

5.2 Vibrational Analysis

Since the vibrational analysis was performed as part of the thermodynamic analysis, the calculated vibrational spectra can be used to understand the modes

responsible for observed IR spectra. The vibrational spectra of the furazan compounds are severely complicated by internal mode coupling. This has led to difficulty interpreting the infrared spectrum of furazans in the past.[16] No previous vibrational analysis of this detail for these compounds is known to us. Due to the reasonable geometries obtained from the calculations based on the accurate replication of the structures obtained by X-ray crystallography (Chapter 4) and the good correlation between calculated and observed spectra, it is felt the assignments of motions are valid. The theoretical frequencies were multiplied by 0.965 as is conventional in DFT. Assignments of modes were made based primarily on patterns and differences in energy levels rather than on exact correlation between calculated and observed spectra. Nevertheless, in many cases the correlation is very good. Where possible, the spectrum used was that of the molecule in the vapor phase from the pyrolysis experiments. In the cases of DAAzF, DAAF, ANAF, DAHzF, and DNHzF, however, no evaporation occurred and comparisons were made with the solid phase spectra obtained from samples pressed as KBr pellets. For the three compounds that were never obtained (DNF, ANAzF, and ANHzF), the motions were also evaluated but no assignments to IR spectra were made. These calculated spectra will be presented as a fingerprint help in the event that these compounds become available.

The molecular motions in some of the modes are quite pure and previous assignments are quite valid. However, in most of the cases, the motions are coupled and there was some difficulty establishing which motion dominates the absorbance. Where practical, a primary mode and one or more coupled modes could be obtained by viewing

the molecular motions in MOLDEN.[17] For each molecule, a numbering scheme is provided (not an IUPAC numbering system) to help make specific assignments. The numbers from the scheme are used as subscripts in the descriptions of motions as needed. If no numbers appear with a motion description, it is implied that each possible motion of that type is active. When two similar motions are active, they are described as either in synchronization (in sync) or out of synchronization (out of sync). In synchronization is the case where any ideal point group is retained. For example, if both carbon-nitrogen double bonds in DAF were stretching at the same frequency and both were stretching simultaneously, this would be described as "in sync." On the other hand, if one were compressing while the other were stretching this would be described as "out of sync." In general, if the two similar motions balance each other, they are "in sync." "Out of sync" is the opposite case. For instance if both amino groups in DAF asymmetrically stretched at the same frequency and both of the "right hand" hydrogen atoms were stretching to the "right" at the same time, they would be "out of sync." In some cases, four similar motions are active and coupled. In these cases the synchronization within each ring is described and then the synchronization between the two rings is described. One special case was the symmetric stretch of the N-O-N portion of the furazan ring. Because it is part of a ring, the mode can be seen as the nitrogen atoms expanding the ring plane, thus lengthening both bonds, or the oxygen atom expanding the ring plane thus lengthening both bonds. As such, special care was taken to specify which motion was intended. Otherwise the description of motions is fairly straightforward. The spectra and

numbering schemes are found in Figures 5.2 – 5.13. The assignment of motions to the frequencies are found in Tables 5.3 – 5.14.

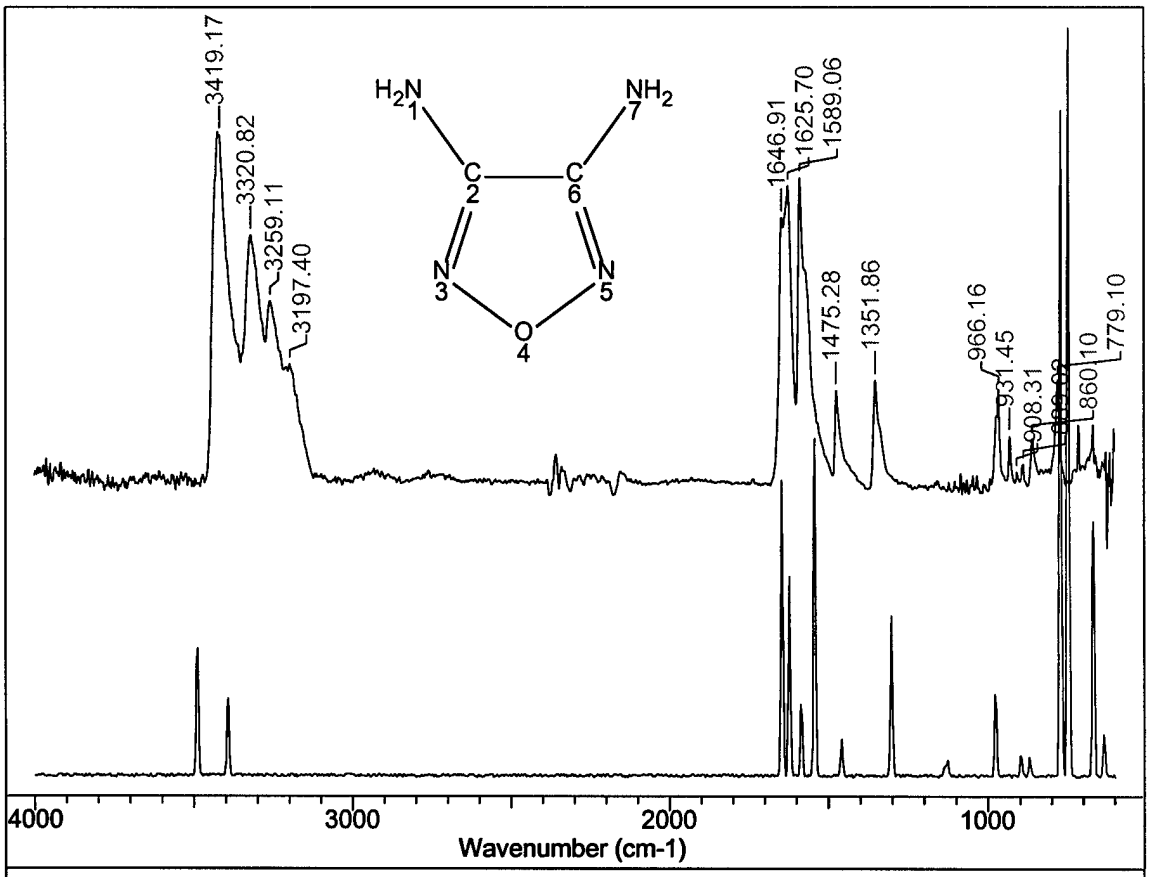

Figure 5.2 Observed (gas phase) and calculated spectrum of DAF

Table 5.3 Assignment of motions to observed infrared peaks for DAF

ν(cm^{-1}) obs	ν(cm^{-1}) calc	Description of major motion from calculation
3425 vs	3490	H-N-H asym. str., in sync
3419 vs	3489	H-N-H asym. str., out of sync
3321 s	3395	H-N-H sym. str., in sync
"	3393	H-N-H sym. str., out of sync
3259 m	-	
3197 m	-	
1647 s	1647	C=N str., out of sync (coupled to H-N-H scissor, out of sync)
1626 s	1624	H-N-H scissor, in sync
1589 s	1586	H-N-H scissor, out of sync (coupled to N=C-N asym. str., out of sync)
1572 s	1545	N=C-N asym. str., In sync
1475 m	1461	C-C str. (coupled to H-N-H in plane wag, in sync)
1352 m	1305	C-N str., out of sync
972 m	979	N-O-N sym. str. (coupled to H-N-H in plane wag, in sync)
966 m	-	
931 w	-	
908 w	898	N-O-N sym. str. (coupled to H-N-H in plane wag, out of sync)
889 w	871	N-O-N sym. str. (coupled to ring breathing)
860 w	-	
779 m	773	N-C-C sym. str., in sync (coupled to ring breathing)

maximum intensity: vs=100-90%, s=90-60%, m=60-30%, w=30-10%, vw<10%

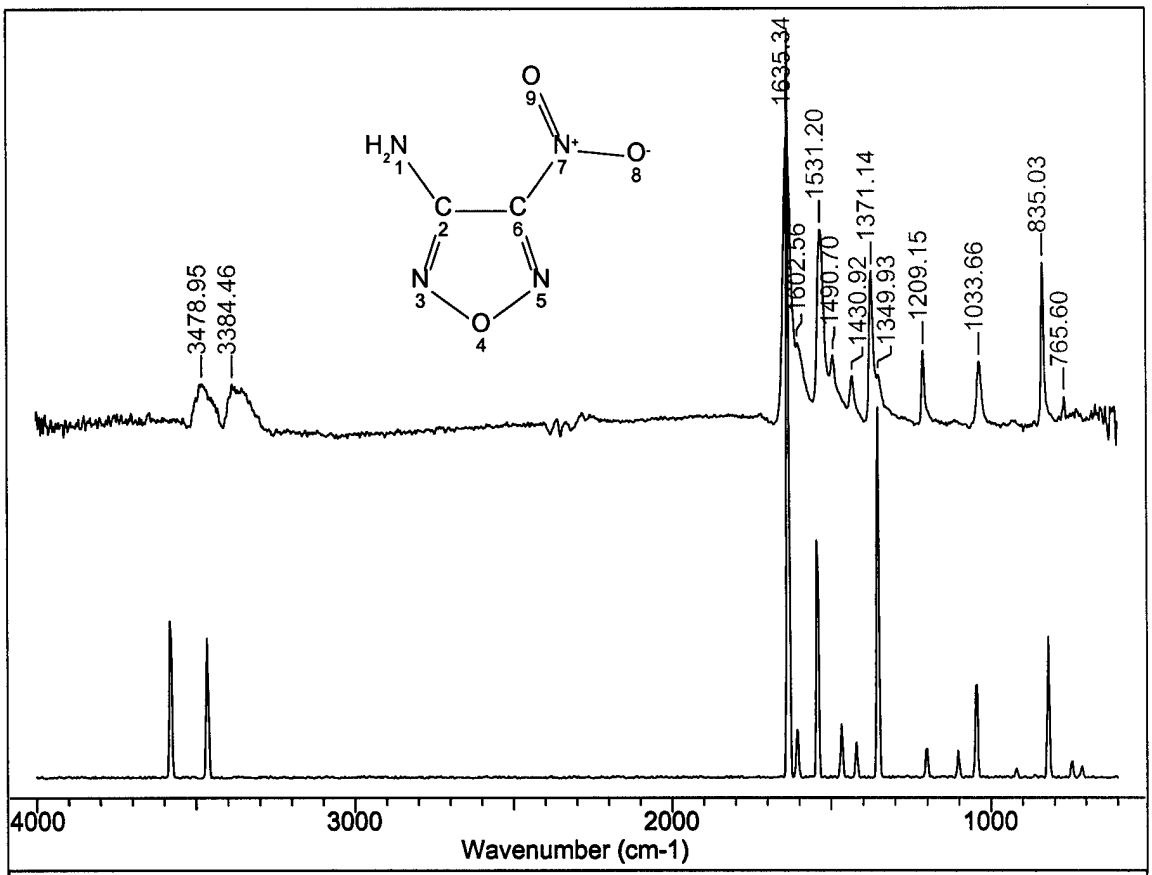

Figure 5.3 Observed (gas phase) and calculated spectrum of ANF

Table 5.4 Assignment of motions to observed infrared peaks for ANF

$\nu(cm^{-1})$		Description of major motion from calculation
obs	calc	
3479 w	3578	H-N-H asym. str.
3384 w	3463	H-N-H sym. str.
1635 vs	1634	N_1-C_2 str. (coupled to H-N-H scissor and O-N-O asym. str.)
1603 m	1606	O-N-O asym. str. (coupled to H-N-H scissor)
1531 s	1542	H-N-H scissor (coupled to O-N-O sym. str.)
1491 w	1468	N_5=C_6-C_2 sym. str. (coupled to N-H in plane wag)
1431 w	1420	N=C-C asym. str., in sync
1371 m	-	
1350 w	1353	C_6-N_7 str. (coupled to O-N-O sym. str.)
1209 m	1202	C_2-C_6-N_7 asym. str.
1034 w	1046	O_4-N_5 str. (coupled to H-N-H in plane wag)
835 m	819	O_4-N_3 str.
766 w	772	N_7-C_6 out of plane bend

maximum intensity: vs=100-90%, s=90-60%, m=60-30%, w=30-10%, vw<10%

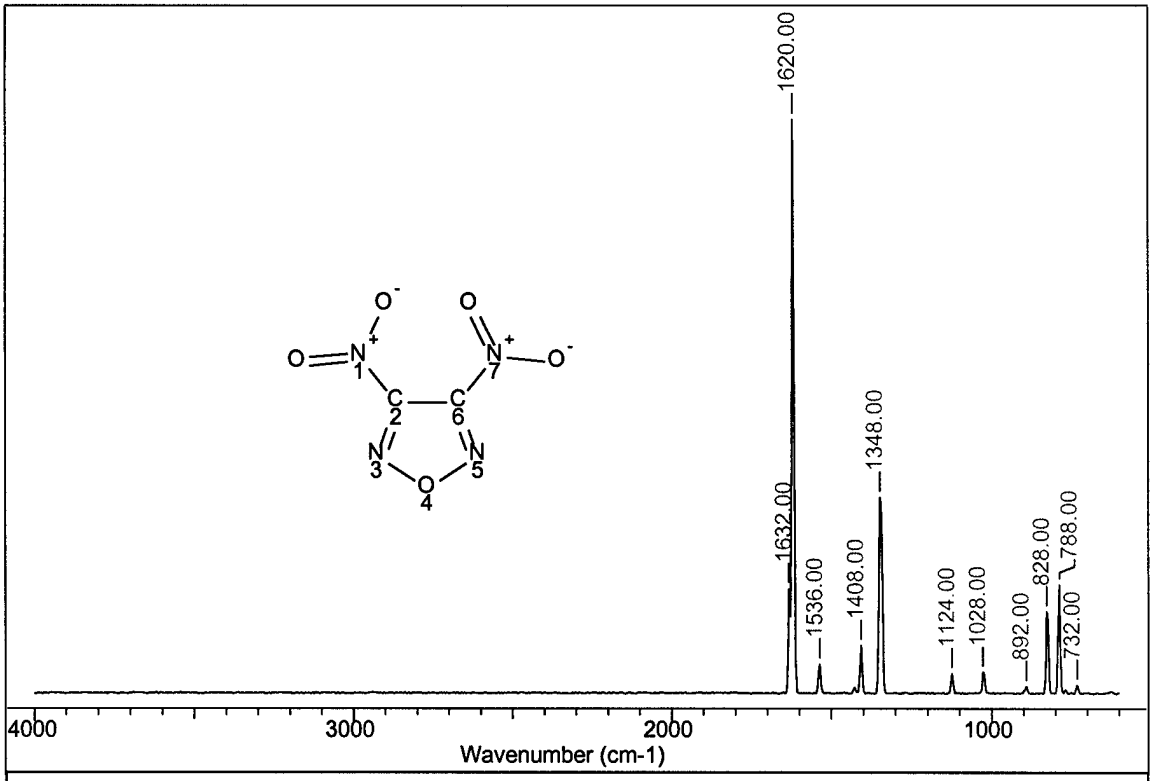

Figure 5.4 Calculated spectrum of DNF

Table 5.5 Assignment of motions to calculated infrared peaks for DNF

$\nu(cm^{-1})$		Description of major motion from calculation
obs	calc	
N/A	1631	O-N-O asym. str., in sync
N/A	1619	O-N-O asym. str., out of sync
N/A	1537	C=N str., out of sync
N/A	1428	C=N str., in sync
N/A	1408	C-C str. (coupled to N-C str.)
N/A	1349	N-C str., out of sync (coupled to O-N-O sym. str.)
N/A	1343	C-C str. (coupled to O-N-O sym. str.)
N/A	1124	N-C str., out of sync (coupled to C=N-O scissor)
N/A	1026	N-O-N sym. str. (O atom moving)
N/A	899	N-O-N asym. str.
N/A	892	N-O-N sym. str. (N atoms moving & coupled to C-C str.)
N/A	826	N-C str., in sync (coupled to O-N-O sym. str. & ring breathing)
N/A	788	C-C=N scissor, out of sync (coupled to O-N-O scissor, out of sync)
N/A	769	N-C-C out of plane bend out of sync
N/A	732	N-C out of plane bend, out of sync
N/A	637	C-C out of plane bend
N/A	625	N-O-N out of plane bend

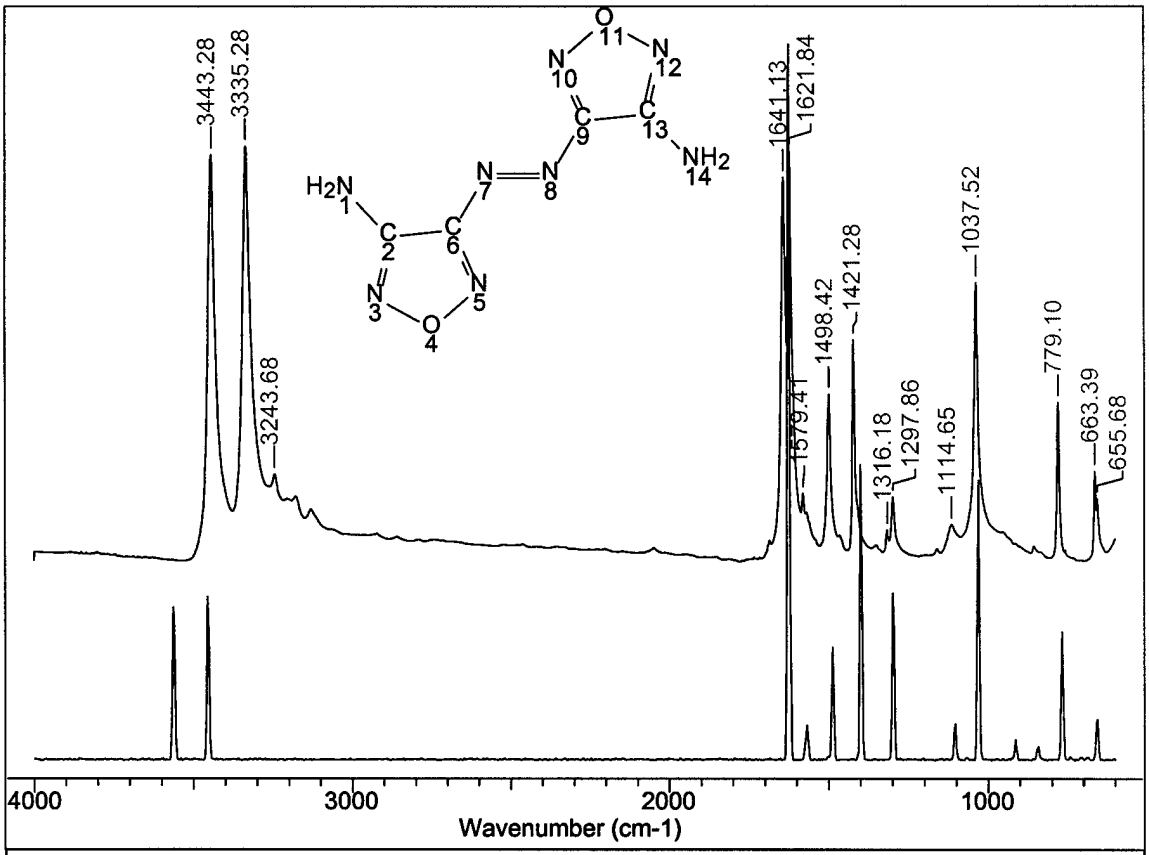

Figure 5.5 Observed (KBr) and calculated spectrum of DAAzF

Table 5.6 Assignment of motions to observed infrared peaks for DAAzF

$\nu(cm^{-1})$		Description of major motion from calculation
obs	calc	
3443 vs	3563	N_1-H asym. str., in sync
"	3562	N_{14}-H asym. str., out of sync
3335 vs	3456	N_1-H sym. str., in sync
"	3455	N_{14}-H sym. str., out of sync
3243 w	-	
1641 vs	1629	H-N-H scissor, in sync
1622 vs	1626	H-N-H scissor, out of sync
1579 w	1573	H-N-H scissor, in sync (coupled to $C_{2,13}$=$N_{3,12}$ str., in sync)
1498 m	1488	C-C str., out of sync (coupled to $C_{6,9}$-$N_{7,8}$ str., out of sync)
1421 m	1399	N-C=N asym. str., each ring in sync but out of sync with each other (coupled to C-C str., out of sync)
1316 vw	-	$N_{7,8}$-$C_{6,9}$=$N_{5,10}$ sym. str., out of sync (coupled to O-N=C scissor, each ring out of sync but in sync with each other)
1298 w	1299	
1115 vw	1106	H-N-H in plane wag, in sync
"	1106	H-N-H in plane wag, out of sync
1038 s	1033	$O_{4,11}$-$N_{5,10}$ str., out of sync (coupled to H-N-H in plane wag, out of sync)
779 m	768	ring breathing, out of sync
663 w	689	entirely coupled molecular breathing
655 w	657	$N_{3,12}$=$C_{2,13}$-$C_{6,9}$ scissor, out of sync

maximum intensity: vs=100-90%, s=90-60%, m=60-30%, w=30-10%, vw<10%

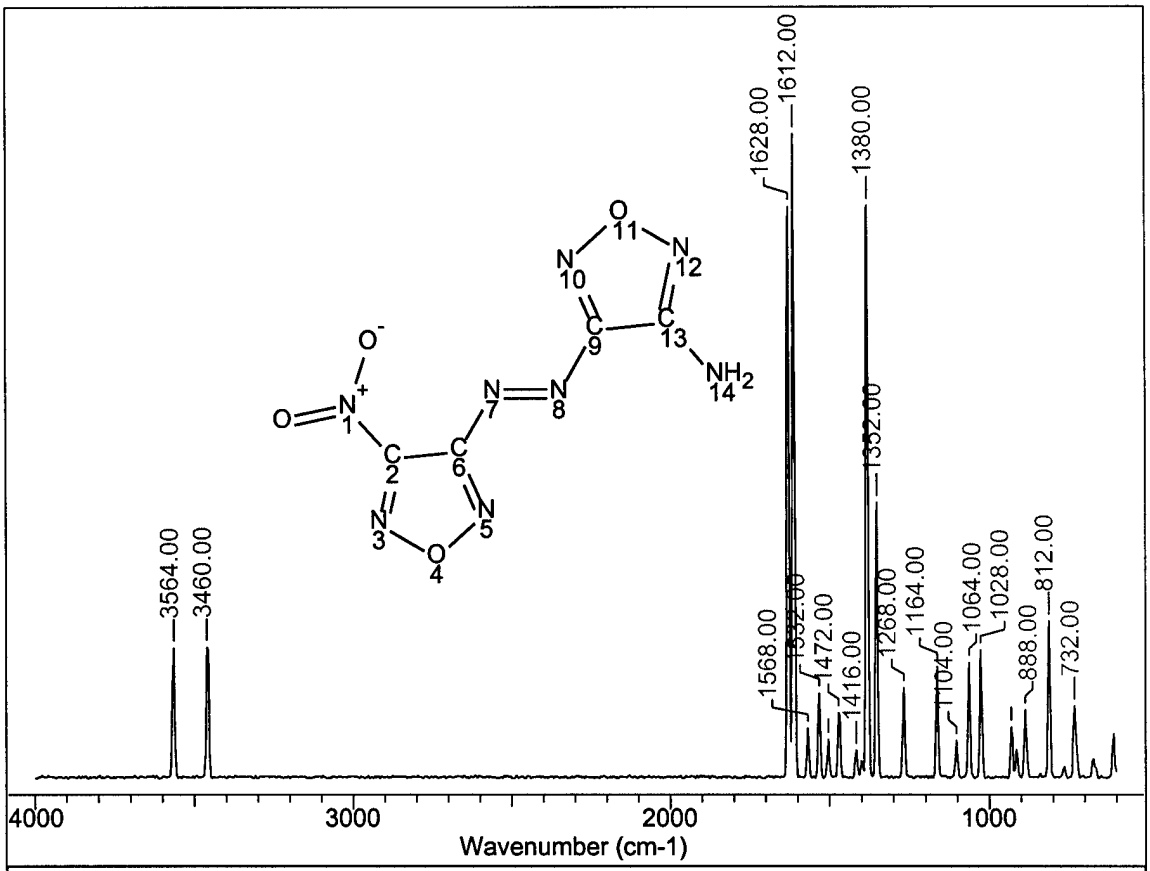

Figure 5.6 Calculated spectrum of ANAzF

Table 5.7 Assignment of motions to calculated infrared peaks for ANAzF

$\nu(cm^{-1})$		Description of major motion from calculation
obs	calc	
N/A	3565	H-N-H asym. str.
N/A	3458	H-N-H sym. str.
N/A	1629	H-N-H scissor (coupled to N_1-C_2 str.)
N/A	1612	O-N-O asym. str.
N/A	1567	H-N-H scissor
N/A	1532	$N_{1,7}$-$C_{2,6}$=$N_{3,5}$ asym. str., out of sync
N/A	1504	N=N str. (coupled to C_9-C_{13} str.)
N/A	1470	C_9-C_{13} str. (coupled to N=N str.)
N/A	1417	C-C str., in sync
N/A	1400	C_2-C_6 str.
N/A	1382	N_{10}=C_9-N_8 asym. str. (coupled to C_2-C_6 str.)
N/A	1353	N_1-C_2 str. (coupled to C_2-C_6 str.)
N/A	1268	N_8-C_9 str.
N/A	1164	N_3=C_2-C_6 scissor, out of sync
N/A	1104	H-N-H in plane wag
N/A	1064	O_{11}-N_{10} str.
N/A	1027	N_3-O_4-N_5 sym. str. (O atom moving)
N/A	931	$C_{2,6}$-$N_{7,8}$=$N_{8,7}$ scissor, in sync (coupled to $O_{11,4}$-$N_{10,5}$ str., in sync)
N/A	889	N_3-O_4-N_5 sym. str. (N atoms moving)
N/A	733	C_6-N_7 str. (coupled to N_7=N_8-C_9 scissor)

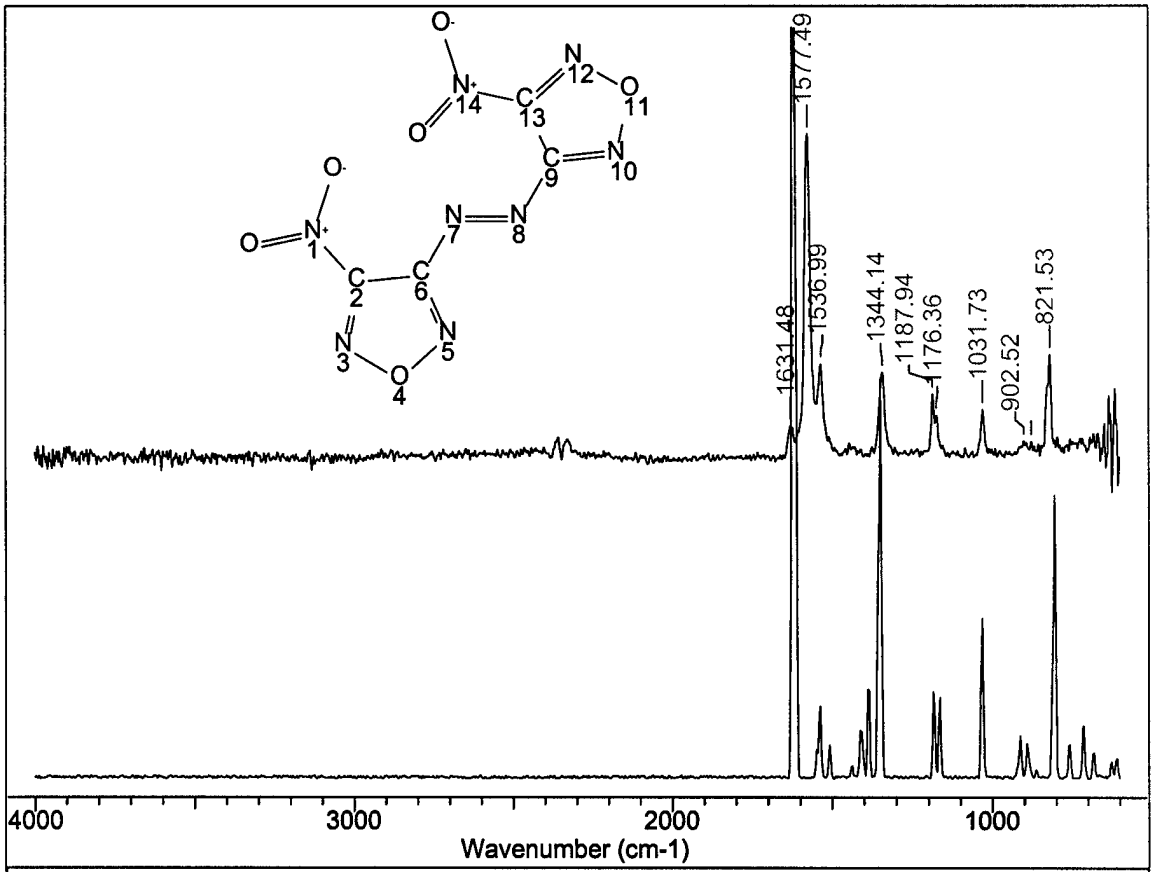

Figure 5.7 Observed (gas phase) and calculated spectrum of DNAzF

Table 5.8 Assignment of motions to observed infrared peaks for DNAzF

$\nu(cm^{-1})$ obs	$\nu(cm^{-1})$ calc	Description of major motion from calculation
1631 w	-	
1577vs	1623	$O\text{-}N_{14}\text{-}O$ asym. str.
"	1614	$O\text{-}N_1\text{-}O$ asym. str.
1537 m	1537	N-C=N asym. str., each ring out of sync and out of sync with eachother
1344 m	1357	$C_9\text{-}C_{13}\text{-}N_{14}$ sym. str.
"	1348	$N_1\text{-}C_2$ str. (coupled to $O\text{-}N_1\text{-}O$ scissor, $C_6\text{-}N_7$ str., and $C_9\text{-}C_{13}$ str.)
1188 w	1182	$N_{1,14}\text{-}C_{2,13}$ str., out of sync (coupled to $C_9\text{-}C_{13}\text{=}N_{12}$ scissor)
1176 w	1165	N=C-C scissor, each ring out of sync and in sync with eachother
1032 w	1034	N-O-N sym. str., out of sync (O atom moving)
903 w	913	N-O-N asym. str., out of sync
879 w	891	$N_3\text{-}O_4\text{-}N_5$ sym. str. (N atoms moving)
822 m	812	O-N-O scissor, out of sync (coupled to ring breathing)

maximum intensity: vs=100-90%, s=90-60%, m=60-30%, w=30-10%, vw<10%

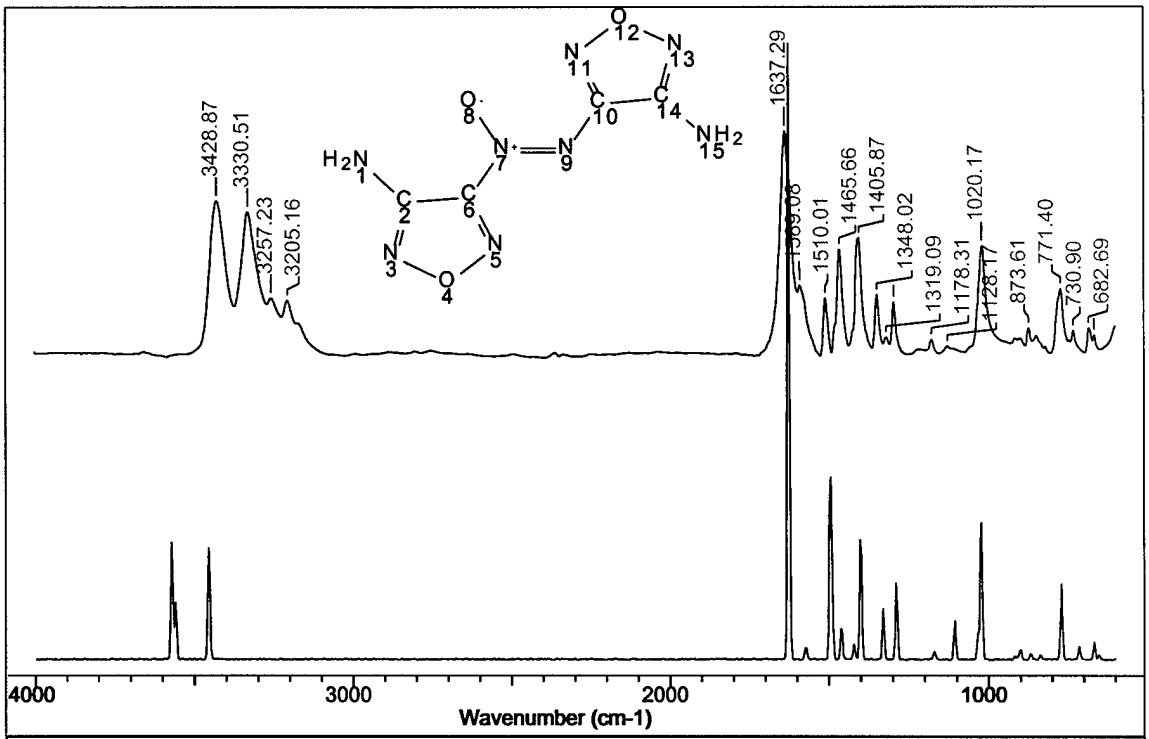

Figure 5.8 Observed (KBr) and calculated spectrum of DAAF

Table 5.9 Assignment of motions to observed infrared peaks for DAAF

$\nu(cm^{-1})$ obs	$\nu(cm^{-1})$ calc	Description of major motion from calculation
3429 s	3571	$H\text{-}N_1\text{-}H$ asym. str.
"	3560	$H\text{-}N_{15}\text{-}H$ asym. str.
3331 s	3456	$H\text{-}N_1\text{-}H$ sym. str.
"	3446	$H\text{-}N_{15}\text{-}H$ sym. str.
3257 w	-	
3205 w	-	
1637 vs	1632	H-N-H scissor, in sync (coupled to $N_{1,15}\text{-}C_{2,14}$ str., out of sync)
"	1628	H-N-H scissor, out of sync (coupled to $N_{1,15}\text{-}C_{2,14}$ str., out of sync)
1589 m	1576	$H\text{-}N_1\text{-}H$ scissor
"	1573	$H\text{-}N_{15}\text{-}H$ scissor
1510 w	1498	N=N str. (coupled to $H\text{-}N_1\text{-}H$ scissor)
1466 m	1462	C-C str., out of sync
1406 m	1402	$C_{10,14}\text{=}N_{11,13}$ str., in sync (coupled to similar weaker motion in other ring)
1348 w	1332	$C_6\text{-}N_7\text{-}O_8$ asym. str. (coupled to $N_7\text{=}N_9\text{-}C_{10}$ scissor)
1319 vw	-	
1296 w	1291	$C_{6,10}\text{-}N_{7,8}$ str., out of sync
1178 vw	1172	$C_2\text{-}C_6\text{-}N_5$ scissor (coupled to N=N str.)
1127 vw	1108	$H\text{-}N_1\text{-}H$ in plane wag
1020 m	1026	$O_{12}\text{-}N_{11}$ str.
874 w	901	$O_{12}\text{-}N_{11}$ str. (coupled to $C_{10}\text{-}C_{14}$ str.)
771 m	772	ring breathing, out of sync
731 w	717	$N_3\text{=}C_2\text{-}C_6$ scissor (coupled to $N_1\text{-}C_2$ str.)
683 w	668	$C_{10,14}\text{-}N_{9,15}$ str., out of sync
665 w	652	$O_8\text{-}N_7\text{=}N_9$ out of plane bend

maximum intensity: vs=100-90%, s=90-60%, m=60-30%, w=30-10%, vw<10%

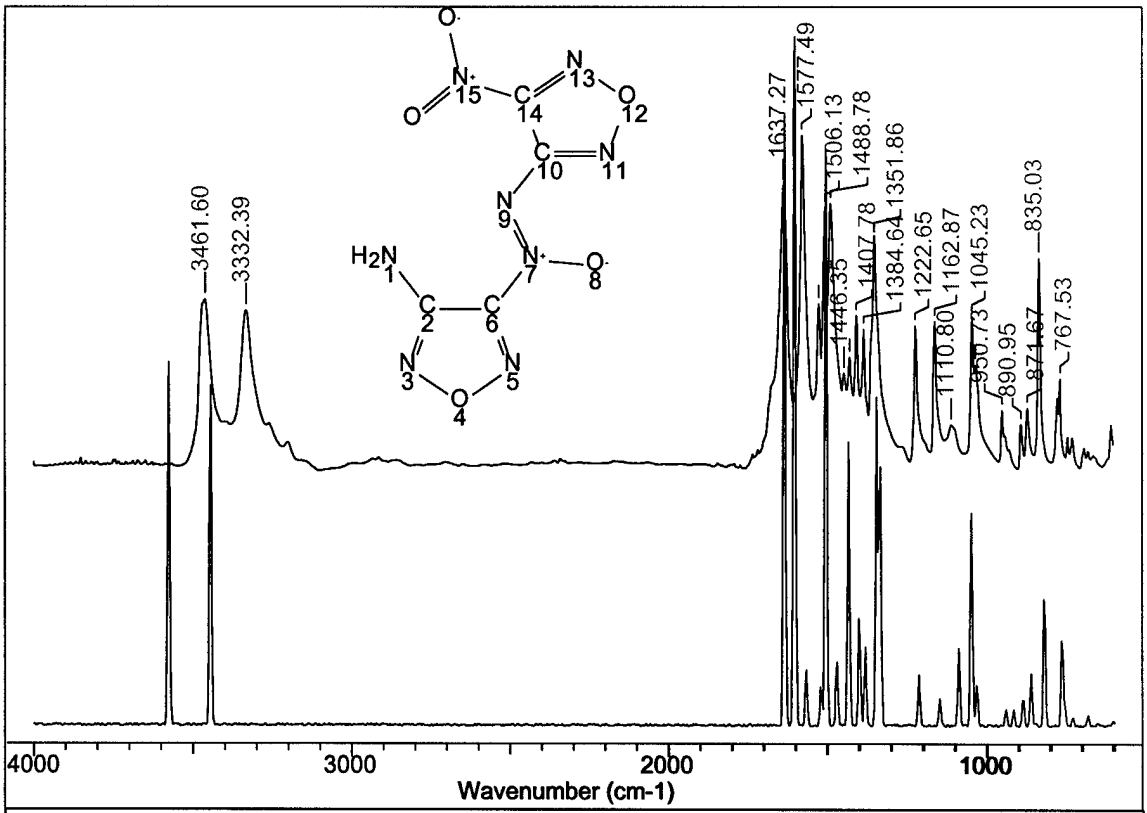

Figure 5.9 Observed (KBr) and calculated spectrum of ANAF

Table 5.10 Assignment of motions to observed infrared peaks for ANAF

$\nu(cm^{-1})$		Description of major motion from calculation
obs	calc	
3462 m	3575	H-N-H asym. str.
3332 m	3445	H-N-H sym. str.
1637 s	1637	N_1-C_2 str. (coupled to N_3=C_2-C_6 sym. str.)
1577 vs	1568	H-N-H scissor
1525 m	1523	$N_{9,15}$-$C_{10,14}$=$N_{11,13}$ asym. str., out of sync
1506 s	1507	N_9=N_7-O_6 asym. str.
1489 s	1473	$N_{3,5}$=$C_{2,6}$-$C_{6,2}$ sym. str., in sync
1446 w	1436	$C_{2,14}$-$C_{6,10}$-$N_{7,9}$ asym. str., in sync
1429 m	-	
1408 m	1403	C_2-C_6 str. (coupled to similar weaker motion in other ring)
1385 m	1384	C_{10}-C_{14} str.
1352 s	1348	N_{15}-C_{14} str. (coupled to O-N-O sym. str. & C_{10}=N_{11} str.)
1223 m	1217	C_6-N_7 str. (coupled to C_{14}-N_{15} str.)
1163 m	1151	C_{14}-C_{10}=N_{11} scissor (coupled to C_2-C_6=N_5 scissor)
1111 w	1091	H-N-H in plane wag
1045 m	1052	O_4-N_5 str. (coupled to H-N-H in plane wag
1034 m	1035	N_{11}-O_{12}-N_{13} sym. str. (O atom moving)
951 w	-	
891 w	890	N_{11}-O_{12}-N_{13} sym. str. (N atoms moving)
872 w	865	N_3-O_4 str.
835 s	823	N_{15}-C_{14} str. (coupled to ring breathing, out of sync)
768 w	766	ring breathing, out of sync

maximum intensity: vs=100-90%, s=90-60%, m=60-30%, w=30-10%, vw<10%

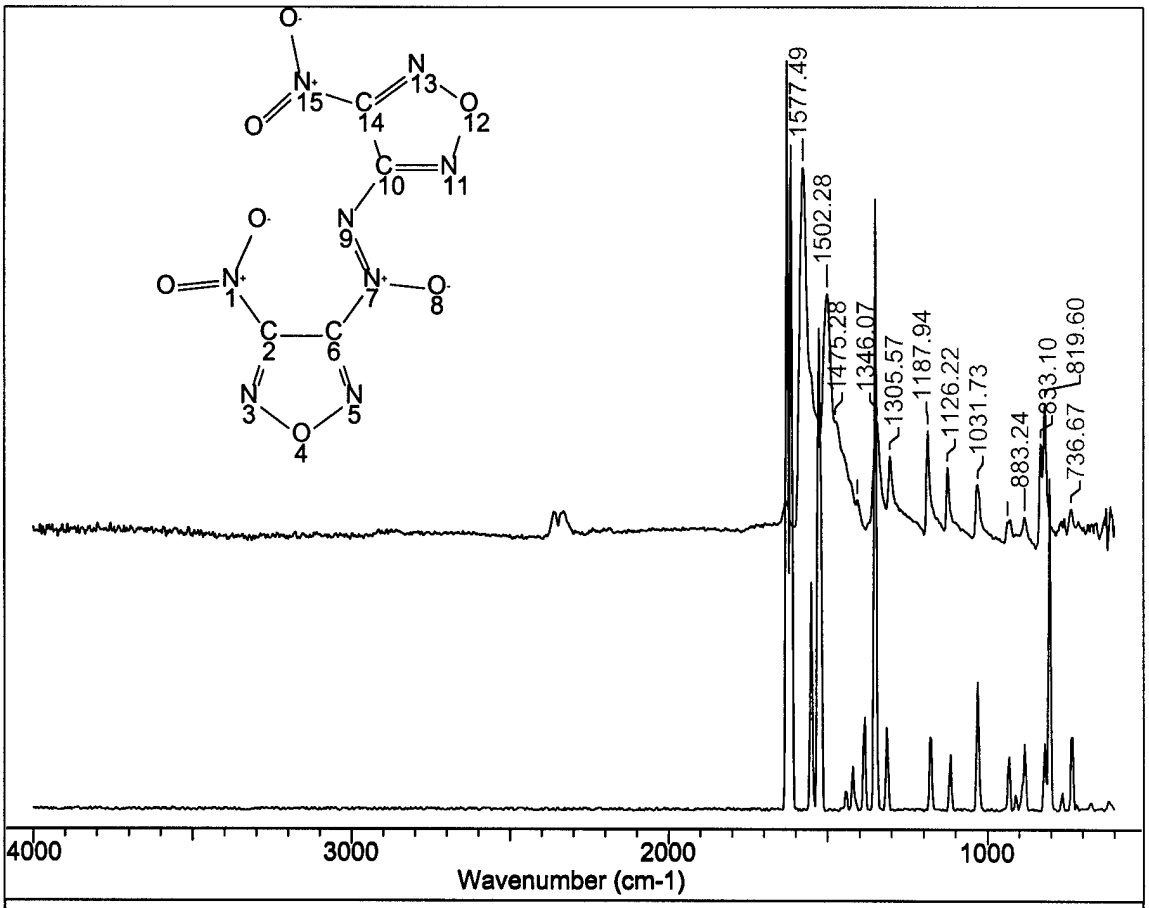

Figure 5.10 Observed (gas phase) and calculated spectrum of DNAF

Table 5.11 Assignment of motions to observed infrared peaks for DNAF

$\nu(cm^{-1})$ obs	$\nu(cm^{-1})$ calc	Description of major motion from calculation
1577 vs	1628	$O\text{-}N_1\text{-}O$ asym. str.
1502 s	1553	$N_{3,5}=C_{2,6}$ str., out of sync
1475 vw	1530	$O_8\text{-}N_7=N_9$ asym. str. (coupled to $N_9\text{-}C_{10}=N_{11}$ asym. str.)
"	1522	$N_{15}\text{-}C_{14}=N_{13}$ asym. str.
1408 w	1385	$C_{10}\text{-}C_{14}$ str. (coupled to similar weaker motion in other ring)
1346 m	1352	$N_1\text{-}C_2$ str. (coupled to $O\text{-}N_1\text{-}O$ sym. str.)
"	1350	$N_{15}\text{-}C_{14}$ str. (coupled to $O\text{-}N_{15}\text{-}O$ sym. str.)
1306 w	1314	$C_2\text{-}C_6\text{-}N_7$ sym. str.
1188 m	1178	$C_{2,14}\text{-}C_{6,10}=N_{3,11}$ scissor, out of sync
1126 w	1117	$N_{3,5}=C_{2,6}\text{-}C_{6,2}$ scissor, out of sync
1032 w	1032	$N_3\text{-}O_4\text{-}N_5$ sym. str. (O atom moving, coupled to similar weaker motion in other ring)
937 vw	933	$N_7=N_9\text{-}C_{10}$ scissor (coupled to $N_{11}\text{-}O_{12}\text{-}N_{13}$ asym. str.)
883 vw	883	$N_{11}\text{-}O_{12}\text{-}N_{13}$ sym. str. (N atoms moving)
833 w	820	$N_{15}\text{-}C_{14}$ str. (coupled to ring breathing, out of sync)
820 m	805	$N_1\text{-}C_2$ str. (coupled to similar weaker motion in other ring)
737 w	733	$N_9\text{-}C_{10}$ str. (coupled to $C_{14}\text{-}C_{10}=N_{11}$ scissor)

maximum intensity: vs=100-90%, s=90-60%, m=60-30%, w=30-10%, vw<10%

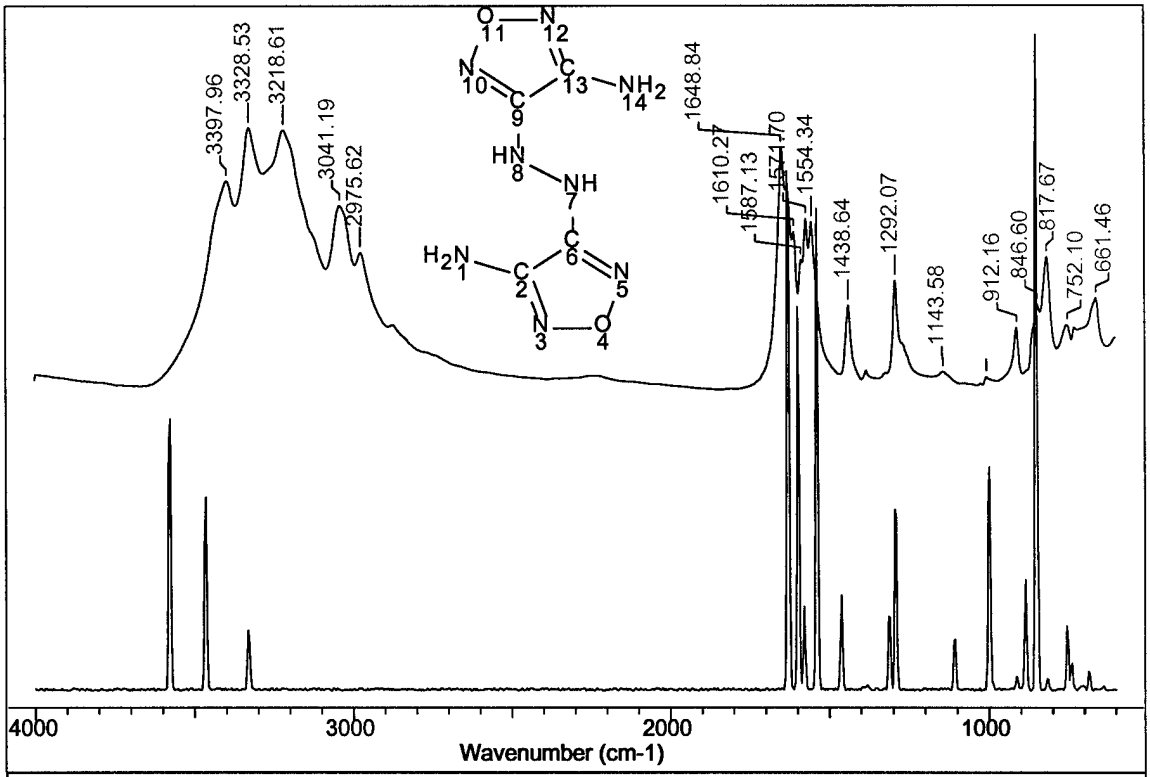

Figure 5.11 Observed (KBr) and calculated spectrum of DAHzF

Table 5.12 Assignment of motions to observed infrared peaks for DAHzF

$\nu(cm^{-1})$		Description of major motion from calculation
obs	calc	
3398 s	3578	H-N-H asym. str., out of sync
"	3577	H-N-H asym. str., in sync
3329 vs	3465	H-N-H sym. str., out of sync
"	3465	H-N-H sym. str., in sync
3219 vs	3332	H-$N_{7,8}$ str., in sync
"	3329	H-$N_{7,8}$ str., out of sync
3041 s	-	
2976 m	-	
1649 vs	1632	N-C=N asym. str., each ring out of sync and out of sync with eachother
1631 vw	1629	N-C=N asym. str., each ring out of sync and in sync with eachother
1610 s	1599	H-N-H scissor, out of sync
1587 m	1581	H-N-H scissor, in sync
1572 s	-	
1554 s	1540	N-C=N asym. str., each ring in sync and out of sync with eachother
1439 m	1463	C-C str., out of sync (coupled to H-$N_{7,8}$) wag
1292 m	1294	N=C-C scissor, each ring out of sync and out of sync with eachother
1146 vw	1110	H-N-H in plane wag, out of sync
1007 vw	1002	N-O-N sym. str. (O atom moving), out of sync
912 w	888	N-O-N sym. str. (N atoms moving), out of sync
847 m	853	H-$N_{7,8}$ out of plane wag, out of sync
818 m	-	
752 w	755	ring breathing, out of sync
661 m	686	C-C out of plane bend, in sync

maximum intensity: vs=100-90%, s=90-60%, m=60-30%, w=30-10%, vw<10%

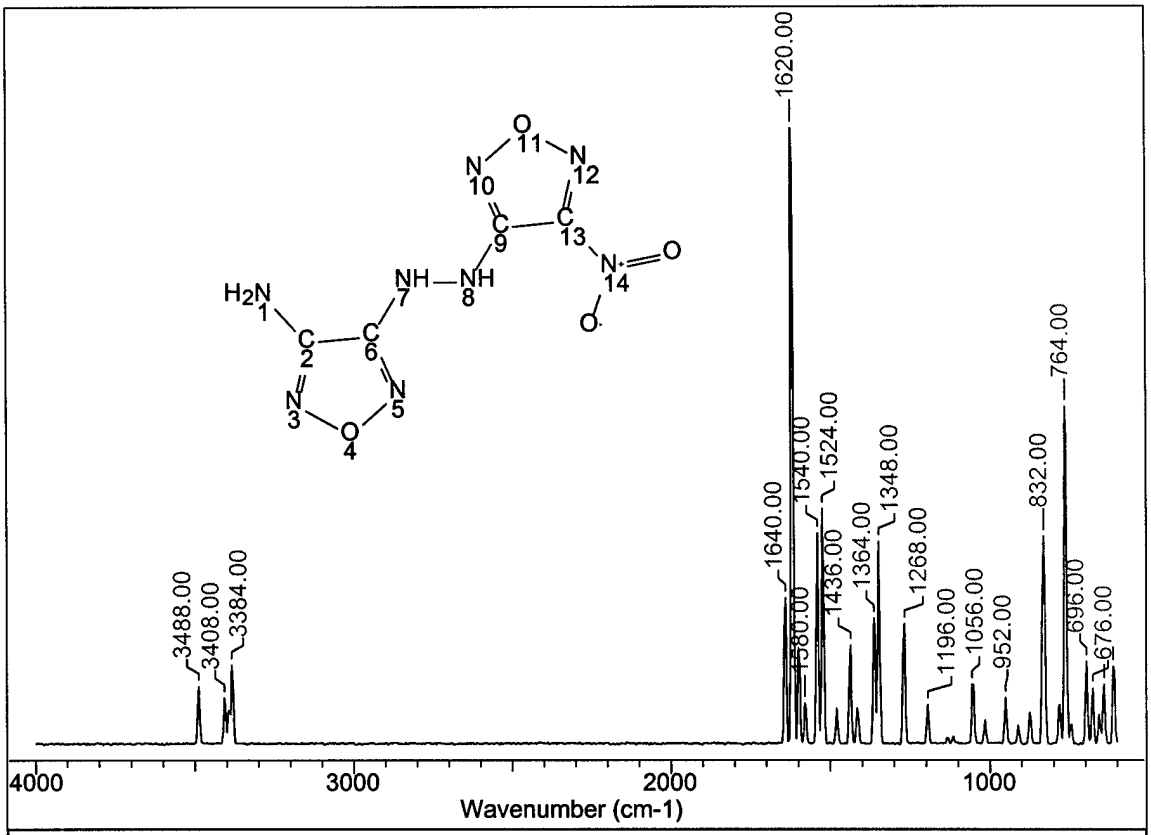

Figure 5.12 Calculated spectrum of ANHzF

Table 5.13 Assignment of motions to calculated infrared peaks for ANHzF

$\nu(cm^{-1})$		Description of major motion from calculation
obs	calc	
N/A	3488	H-N-H asym. str.
N/A	3406	H-N_7 str.
N/A	3394	H-N-H sym. str.
N/A	3382	H-N_8 str.
N/A	1641	H-N-H scissor
N/A	1618	O-N-O asym. str.
N/A	1579	O-N-O asym. str. (coupled to C_9-N_8 str.)
N/A	1540	$N_{3,5}$=$C_{2,6}$-$C_{6,2}$ asym. str., in sync
N/A	1523	H-N_8 in plane wag
N/A	1437	$N_{10,12}$=$C_{9,13}$-$C_{13,9}$ asym. str., in sync
N/A	1362	H-N_8 in plane wag (coupled to C_9-C_{13} str.)
N/A	1348	C_9-C_{13} str. (coupled to O-N-O sym. str. & H-N_8 in plane wag)
N/A	1269	C_2-C_6=N_5 sym. str.
N/A	1196	N_{10}=C_9-N_8 sym. str. (coupled to N_{10}=C_9-C_{13} sym. str.)
N/A	1054	N_{10}-O_{11}-N_{12} sym. str. (O atom moving)
N/A	951	N_{10}-O_{11}-N_{12} asym. str.
N/A	835	O_4-N_5 str. (coupled to C_6-N_7 str.)
N/A	829	ring breathing (9--13 ring only)
N/A	762	H-N-H out of plane bend
N/A	697	N_1-C_2-C_6 out of plane bend
N/A	677	C_2-C_6 out of plane bend (coupled to C_2-C_6 str.)
N/A	642	$C_{6,9}$-$N_{7,8}$ str., out of sync
N/A	610	H-$N_{7,8}$ out of plane wag, in sync

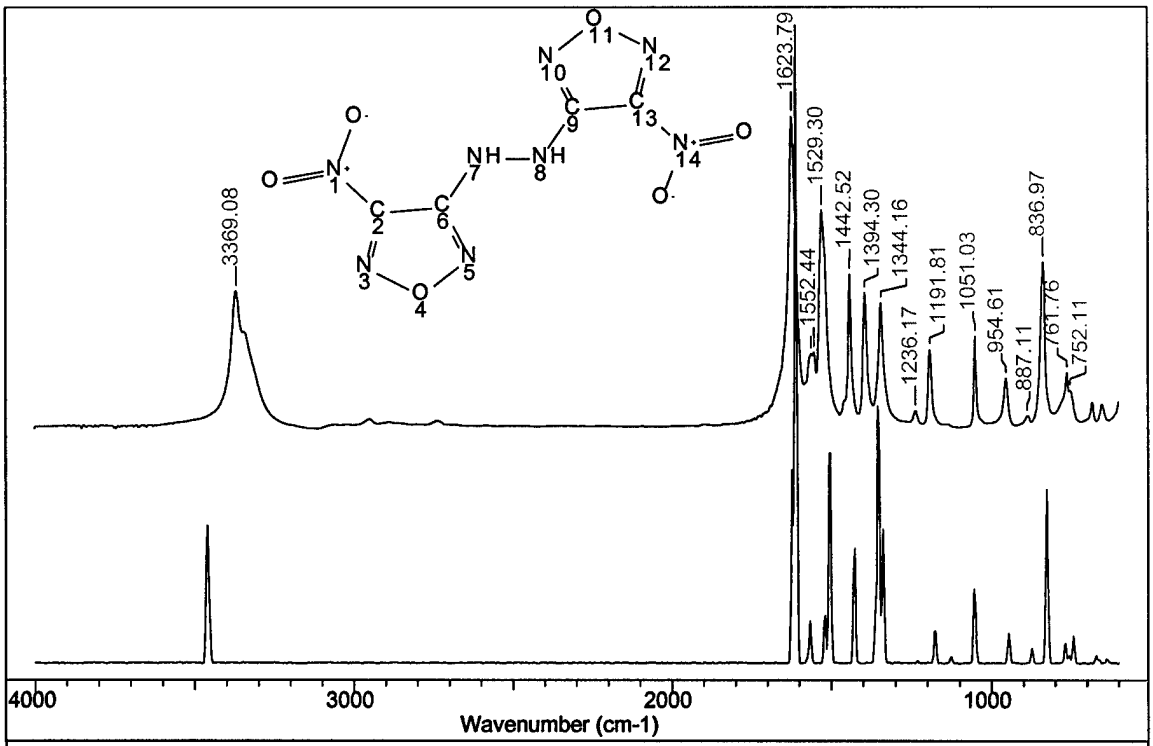

Figure 5.13 Observed (KBr) and calculated spectrum of DNHzF

Table 5.14 Assignment of motions to observed infrared peaks for DNHzF

$\nu(cm^{-1})$ obs	$\nu(cm^{-1})$ calc	Description of major motion from calculation
3369 m	3461	H-N str., out of sync
"	3455	H-N str., in sync
1624 vs	1623	O-N-O asym. str., in sync (coupled to N=C str., each ring out of sync and in sync with eachother)
"	1612	O-N-O asym. str., out of sync (coupled to N=C str., each ring out of sync and out of sync with eachother)
1562 w	1567	N-C=N asym. str., each ring out of sync and out of sync with eachother
1552 w	1522	H-N in plane wag, in sync
1529 s	1505	H-N in plane wag, out of sync
1443 m	1429	N-C=N asym. str., each ring in sync and out of sync with eachother
1394 m	1364	C-C str., in sync (coupled to H-N in plane wag, in sync)
"	1354	H-N in plane wag, out of sync (coupled to O-N-O sym. str., in sync)
"	1354	H-N in plane wag, in sync (coupled to O-N-O sym. str., in sync & $N_{1,14}$-$C_{2,13}$ str.,
1344 m	1339	H-N in plane wag, out of sync (coupled to C-C str., out of sync)
1236 vw	-	
1192 w	1178	C-C=N sym. str., out of sync
1051 w	1056	$N_{3,12}$-$O_{4,11}$ str., out of sync
"	1053	$N_{3,12}$-$O_{4,11}$ str., in sync
955 w	948	N-O-N asym. str., in sync
887 vw	874	$N_{5,10}$-$O_{4,11}$ str., out of sync
"	874	$N_{5,10}$-$O_{4,11}$ str., in sync
837 m	829	$N_{5,10}$-$O_{4,11}$ str., out of sync (coupled to O-N-O scissor, out of sync)
"	826	$N_{5,10}$-$O_{4,11}$ str., in sync (coupled to O-N-O scissor, in sync)
762 w	770	$C_{6,9}$-$N_{7,8}$ str., out of sync
752 vw	744	$N_{1,14}$-$C_{2,13}$-$C_{6,9}$ out of plane bend, in sync

maximum intensity: vs=100-90%, s=90-60%, m=60-30%, w=30-10%, vw<10%

5.3 References

1. Chavez, D.; Hill, L.; Hiskey, M.; and Kinkead, S., J. Energet. Mat., (1999) in press.

2. Sinditskii, V. P.; Dong, H. W.; Serushkin, V.; Fogelzang, A. E.; and Sheremetev, A. B., Int. Ann. Conf. ICT, 29th (Energetic Materials), *170-1*, (1998).

3. Sheremetev, A. B.; Kulagina, V. O.; Aleksandrova, N. S.; Novikova, T. S.; and Khmel'nitskii, L. I., Proc. Beijing Int. Symp. Pyrotech., *249,* (1995).

4. Sheremetev, A. B.; Kulagina, V. O.; Aleksandrova, N. S.; Dmitriev, D. E.; Strelenko, Y. A.; Lebedev, V. P.; and Matyushin, Y. N., Prop. Explos. Pyrotech., **23**, *142,* (1998).

5. Son, S. F.; Berghout, H. L.; Bolme, C. A.; Chavez, D. E.; Naud, D.; and Hiskey, M. A., 1999 JANNAF PSHS Meeting, Cocoa Beach, FL, October 18-22, (1999).

6. Lou Cannizzo, Thiokol Corp., Brigham City, UT, personal communication (1999).

7. Frisch M. J.; Trucks G. W.; Schlegel H. B.; Scuseria G. E.; Robb M. A.; Cheeseman J. R.; Zakrzewski V. G.; Montgomery J. A. Jr.; Stratmann R. E.; Burant J. C.; Dapprich S.; Millam J. M.; Daniels A. D.; Kudin K. N.; Strain M. C.; Farkas O.; Tomasi J.; Barone V.; Cossi M.; Cammi R.; Mennucci B.; Pomelli C.; Adamo C.; Clifford S.; Ochterski J.; Petersson G. A.; Ayala P. Y.; Cui Q.; Morokuma K.; Malick D. K.; Rabuck A. D.; Raghavachari K.; Foresman J. B.; Cioslowski J.; Ortiz J. V.; Stefanov B. B.; Liu G.; Liashenko A.; Piskorz P.; Komaromi I.; Gomperts R.; Martin R. L.; Fox D. J.; Keith T.; Al-Laham M. A.; Peng C. Y.; Nanayakkara A.; Gonzalez C.; Challacombe M.; Gill P. M. W.; Johnson B.; Chen W.; Wong M. W.; Andres J. L.; Gonzalez C.; Head-Gordon M.; Replogle E. S.; Pople J. A., Gaussian, Inc., Pittsburgh PA, 1998.

8. Lee, C.; Yang, W.; and Parr, R. G., Phys. Rev. B, **37**, *785*, (1988).

9. Becke, A. D., J. Chem. Phys., **104**, *1040*, (1996).

10. Cox, J.D., and Pilcher, G., Thermochemistry of Organic and Organometallic Compounds, Academic Press, New York, *1-636*, (1970).

11. Lebedeva, N.D., and Ryadenko, V.L.R., Russ. J. Phys. Chem. (Engl. Trans.), **47**, *1382*, (1973).

12. Lemoult, M.P., Ann. Chim.Phys., **12**, *395-432,* (1907).

13. Smith, N.K., and Good, W.D., J. Chem. Eng. Data, **12**, *572-574*, (1967).

14. Kunyavskaya, S.G.; Karyakin, N.V.; Krylova, G.P.; Chernova, V.I.; and Rabinovich, I.B., Tr. Khim. Khim. Tekhnol., *58-59*, (1973).

15. Nishiyama, K., and Sakiyama, M.; Seki, S., Bull. Chem. Soc. Jpn., **56**, *3171-3172*, (1983).

16. Stoner, C. E. Jr. and Brill, T. B., Combust. Flame, **83**, *302*, (1991).

17. Schaftenaar, G., and Noordik, J.H., J. Comput.-Aided Mol. Design, **14** *123-134,* (2000)